



The evolution of the subcontinental mantle beneath the Central Iberian Zone: Geochemical tracking of its mafic magmatism from the Neoproterozoic to the Cenozoic

C. Villaseca^{a,b,*}, D. Orejana^a, P. Higuera^c, C. Pérez-Soba^a, J. García Serrano^a, S. Lorenzo^c

^a Dpto. Mineralogía y Petrología, Facultad CC Geológicas, Universidad Complutense (UCM), 28040 Madrid, Spain

^b Instituto de Geociencias IGEO (UCM, CSIC), 28040 Madrid, Spain

^c Dpto. Ingeniería Geológica y Minera, IGeA, Universidad de Castilla-La Mancha, 13400 Almadén (Ciudad Real), Spain

ARTICLE INFO

Keywords:

Central Iberian Zone
Cadomian and Variscan orogenies
Nd-Sr-Pb isotopes
Mantle-derived magmatism
Subcontinental mantle evolution
European basement terranes

ABSTRACT

Continental lithosphere is modified over eons in response to large-scale tectonic processes, such as rifting and collisions. The lithospheric mantle beneath central Iberia was affected by multiple Neoproterozoic to Cenozoic events including two orogenic cycles. However, the details of this evolution, and the relationship of the Iberian lithosphere to that beneath central Europe remains poorly constrained. We have compiled a trace element and isotope (Sr-Nd-Pb) data set ($n = 230$) regarding the main ten mafic magmatic episodes that intruded the central-western Iberia basement during a 575 Ma age range. In this long period, two orogenic events with accompanying mafic calc-alkaline magmatism (Cadomian and Variscan cycles) were followed by eight intraplate, alkaline or tholeiitic, magmatic inputs. The two orogenic episodes have subordinate mafic intrusions associated to a more voluminous felsic magmatism, which highlights both the major intracrustal recycling promoted and the significant crustal thickening accompanying these convergence tectonic events. Nevertheless, only minor crustal subduction signatures within deep mantle are observed in mafic magmas or mantle xenoliths after those two orogenic cycles, and the existence of an old (pre-Neoproterozoic) enriched subcontinental mantle beneath central Iberia is suggested. Mantle-derived magmas from central European basement terranes (Bohemian to Armorican-French Massif Central massifs) show a marked contrast of geochemical tracers during the same long time record. They show more juvenile and depleted mantle sources during the pre-Variscan times indicating their farther distance to continental Gondwana than the studied central Iberian terrane. Thus, the change in Nd isotopes and model ages associated with the Variscan orogeny is more abrupt in central European terranes. This collisional event was followed by the arrival of broadly similar mafic magmas in both southwestern and central European terranes, implying substantial crust-mantle interaction across a wide geographical area. The post-Variscan mafic magmatism, mainly from Cretaceous time, suggests a lithospheric mantle rejuvenation by widespread asthenospheric upwelling throughout these western circum-Mediterranean areas. However, the presence of minor episodes of intraplate K-rich alkaline magmatism involving enriched lithospheric mantle sources in the southernmost Mediterranean Europe marks a contrast, suggesting a complex lithospheric/asthenospheric mantle flow regime in these areas during post-collisional convergence between Africa and Eurasia.

1. Introduction

The comparison of geochemical and isotopic signatures of mantle-derived magmas over a long time span, involving collisional and extensional tectonic events, sheds light on the extent of crust-lithospheric/asthenospheric mantle interactions during and after orogenesis. In this respect, studies comparing the magmatic characteristics of

igneous suites varying through time in the same terrane or crustal block of the Western Europe (e.g., Dostal et al., 2019a, 2019b; Krmíčková et al., 2020) have provided important insights. The review of the different mafic igneous rocks outcropping in the Iberian basement from Late Neoproterozoic to the Cenozoic can also contribute to a better understanding of the evolution of the subcontinental mantle in Western Europe and its interaction with the crust during the assemblage of the

* Corresponding author.

E-mail address: granito@ucm.es (C. Villaseca).

<https://doi.org/10.1016/j.earscirev.2022.103997>

Received 14 October 2021; Received in revised form 7 February 2022; Accepted 14 March 2022

Available online 17 March 2022

0012-8252/© 2022 The Authors. Published by Elsevier B.V. This is an open access article under the CC BY-NC-ND license (<http://creativecommons.org/licenses/by-nc-nd/4.0/>).

Gondwana and Pangea supercontinents and their subsequent breakdown.

Previous studies on Late Neoproterozoic to Cenozoic mafic rocks of the Bohemian Massif (Dostal et al., 2019a), later extended to most of the European Variscan Belt (Dostal et al., 2019b), highlight the abrupt geochemical change in mafic magmatism in most of the central-Europe terranes associated with the Variscan orogeny, suggesting that this orogenic event triggered an extensive crust-mantle interaction process. The study of the chemical tracking of mantle inputs into crustal blocks allows additional insights in the geodynamic evolution and paleogeographical approaches of basement terranes.

Some approaches have been done in Iberia to establish secular variations of mafic magmatism through the Paleozoic, mostly within central Spain. Villaseca et al. (2004) and Orejana et al. (2020) have described at least six mantle-derived magmatic events representing inputs into the continental crust of the Spanish Central System, from tholeiitic metabasites (473–453 Ma) to the emplacement of the Messejana-Plasencia dyke (203 Ma), associated to the Central Atlantic Magmatic Province (CAMP), also of tholeiitic affinity. Most of the mafic magmatism discussed in the above studies implies melting of lithospheric sources, variably enriched due to crustal material subducted during the Late Cadomian (540–480 Ma) and the Variscan (360–285 Ma) orogenic cycles. The input of basic to ultrabasic alkaline magmas from a deep asthenospheric mantle source during the Upper Permian is interpreted as an alkaline event precursor of the Atlantic Ocean protorifting (Orejana et al., 2008). Additionally, Gutiérrez-Alonso et al. (2011) examine the impact of the Variscan orogeny in the evolution of mantle sources of Iberian mafic rocks from pre-Variscan to present, using published Nd isotopic data. They suggest that the incoming of post-Variscan asthenospheric magmas are mostly due to delamination of the Variscan lithosphere during and after the bending of this orogenic belt into orocline, thus revising the model of extensional upwelling of hot asthenospheric mantle initially exposed by Orejana et al. (2008).

This study aims to systematize the chemical evolution of the mantle-derived magmatism in central Iberia from the Neoproterozoic to Cenozoic times. To do this, we provide new data on these magmatic rocks which add to the abundant geochemical, isotopic and geochronological data published during the last decades. To our knowledge, this is the first attempt to get a comprehensive characterization and discussion of the main geochemical, petrogenetic and geodynamic features of the 10 successive mafic magma suites outcropping in central-western Iberia. Our main objective is to track and interpret the evolution of the mantle sources beneath the Central Iberian Zone (CIZ) and neighbouring areas. We have excluded data on mafic magmatism outside the CIZ, those from other Iberian peri-Gondwanan terranes that clearly had a different paleogeographical position during pre-Variscan times (e.g., Ossa Morana and Galicia-Trás-os-Montes Zones, OMZ and GTMZ, respectively). Nevertheless, the timing of the CIZ-OMZ accretion is still a debatable issue and some studies suggest an early OMZ accretion during the Cadomian orogeny (e.g., Ribeiro et al., 2007; Sánchez García et al., 2019). Significant differences in the Cadomian magmatism and the Nd model ages of Ediacaran-Ordovician metasedimentary rocks from these terranes suggest a more westerly low Paleozoic paleogeographical position of the OMZ when compared to the CIZ (Stampfli et al., 2013; Cambeses et al., 2017). This is also in agreement with differences in the sedimentary features of Ordovician sequences between both zones (Gutiérrez-Marco et al., 2002). Accordingly, we consider that it was during the Variscan collision that these terranes were accreted to form the Iberian Massif. Thus, assembled terranes (at least, the central-western half of the Iberian Massif) share the same geodynamic position and variably record the successive later minor mafic magmatic events from the Permian to the Cenozoic. We have also included recent analyses on the Pliocene volcanism from the Calatrava Volcanic Field (e.g., Villaseca et al., 2020). The whole data set covers an overall time range of nearly 575 Ma of mantle-derived magmatism in central Iberia. This compilation offers an updated overview of the evolution of the

continental lithosphere in central Iberia that can serve as a basis for future comparative studies with other circum-Mediterranean Variscan terranes. The evolution of mantle sources pointed out in this work helps to unravel the role played by crustal recycling and entrainment of sublithospheric components in the Iberian lithospheric mantle during such a wide age range, thus leading to an improved discussion of their correlation with the established tectonic events.

2. Geological setting

The CIZ is a basement region exposing one of the largest European Variscan granitic batholiths intrusive in thick sequences of metamorphic rocks. It represents the innermost region of the Variscan Iberian Belt (Fig. 1), and it is consequently interpreted as the Iberian Autochthonous terrane (Quesada, 1991). The metamorphic rocks consist of: (i) meta-sedimentary sequences deposited in an active continental margin during the Cadomian convergent orogenic cycle (Neoproterozoic–Cambrian) and in the context of a later passive margin (Ordovician to Devonian), and (ii) Cambrian–Ordovician metagranitic orthogneisses mostly dated at 496–478 Ma (e.g., Rubio-Ordóñez et al., 2012; Villaseca et al., 2016).

The magmatic events recorded in the CIZ might be ascribed to six main stages: (1) the Cadomian orogeny (e.g., Bandrés et al., 2004; Villaseca et al., 2016), (2) the Ordovician to Devonian passive margin stage (e.g., Orejana et al., 2017; Gutiérrez-Marco et al., 2019), (3) the collisional Variscan cycle (e.g., Bea et al., 1999; Orejana et al., 2009; Scarrow et al., 2009), (4) the Permian extension (e.g., Orejana et al., 2008; Scarrow et al., 2011), (5) the Triassic–Jurassic rifting leading to the opening of the Atlantic ocean (e.g., Cebriá et al., 2003), and (6) the Mesozoic to Cenozoic alkaline intraplate magmatism (e.g., Mata et al., 2015; Grange et al., 2010; Ancochea and Huertas, 2021). Felsic crustal magmas dominate during the two orogenic events (Cadomian and Variscan), when mantle-derived magmas are clearly subordinate (< 5 vol% of magma inputs), whereas mafic melts represent the main magmatism (up to 100 vol% of lithotypes) in the alkaline or tholeiitic magma series intruding during the extensional periods between subduction (convergent and collisional) stages (Fig. 2). These mafic suites include small plutonic bodies, subvolcanic (dyke swarms) and volcanic mantle-derived rocks (Fig. 1). The estimation of the total volume of mantle-derived magmas added during the last 575 Ma to the CIZ upper crust is nevertheless extremely low (< 1 vol%) when compared to the huge crustal-derived felsic peraluminous magmatism intruded during the two orogenic cycles. In addition, according to the scarce volume of mafic granulites from the central Iberian lower crust sampled by post-Variscan alkaline magmas (Villaseca et al., 1999; Puelles et al., 2019), no significant mafic underplating was coevally produced, suggesting a minor growth of the continental crust of central Iberia during such a long period of time. The main petrological, geochemical and geochronological features of the studied mafic rocks are summarized in Table 1.

The oldest mafic magmatic rocks from the CIZ correspond to Late Neoproterozoic to early Paleozoic calc-alkaline intrusives, which cannot be unambiguously ascribed to this terrane as they outcrop close to the debatable boundary with the OMZ (CALC-1, Fig. 1). These are the Mérida ultrabasic to acid (cumulate gabbros and hornblendites to granodiorites) igneous complex of 570–580 Ma (Bandrés et al., 2004) and the gabbro-to-granodiorite Carrascal massif of 486–471 Ma (Solá et al., 2010). During the Cambrian–Early Ordovician, a voluminous felsic magmatism intruded into the upper crustal levels of the CIZ generating two coeval subparallel belts of granitoids. The most external one, located to the plate edge at that time (towards the current OMZ boundary), is the southern CIZ tonalite-granodiorite belt, mostly of I-type granite composition (e.g., Antunes et al., 2009; Rubio-Ordóñez et al., 2012). On the contrary, in the northern CIZ, a more voluminous and felsic batholithic belt (granodiorite to leucogranite), constituted by highly peraluminous S-type granites, intruded into the innermost continental metasedimentary sequences of this terrane (Villaseca et al., 2016). No mafic magmas coexisted with this huge Early Ordovician

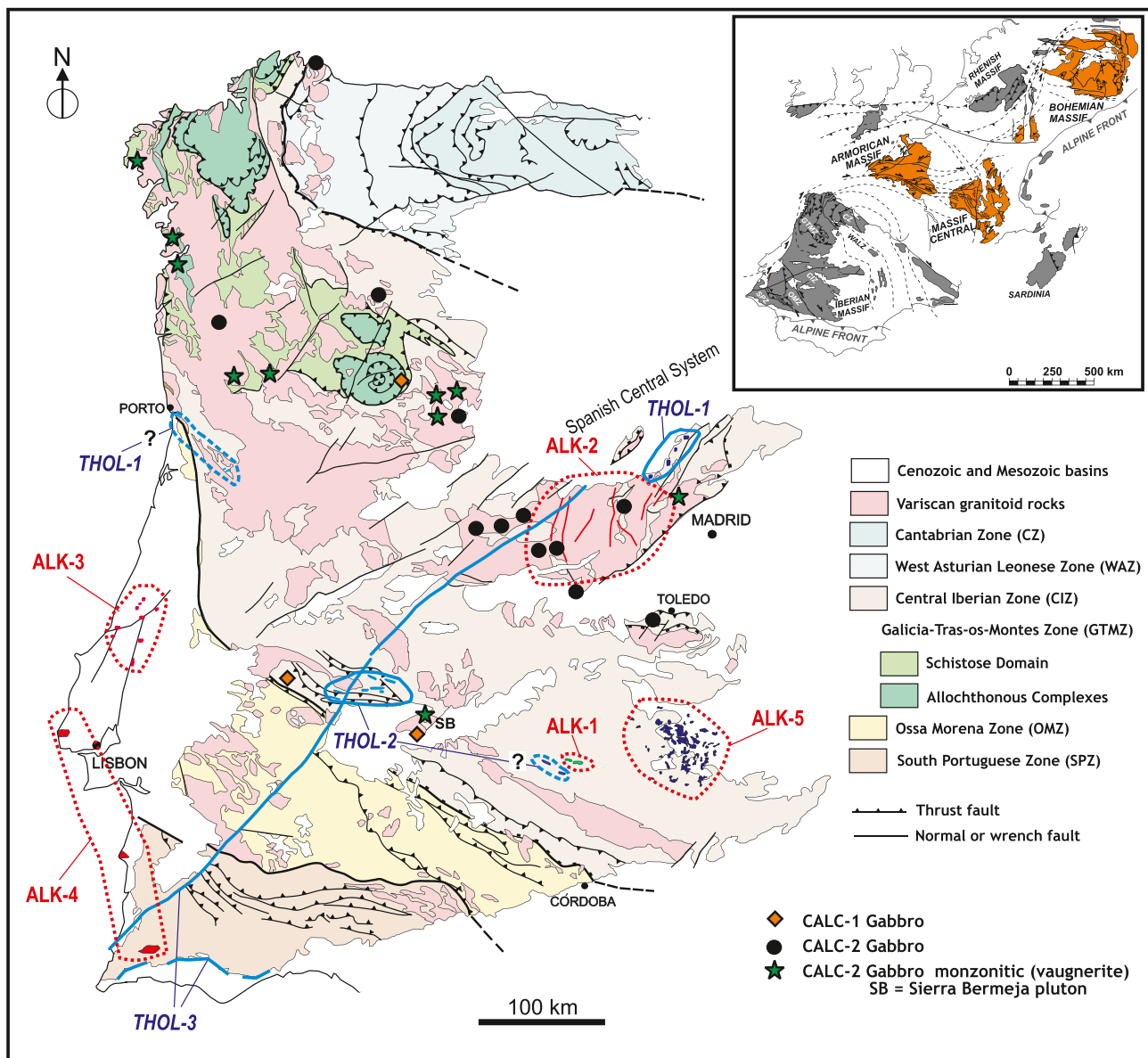


Fig. 1. Geological map showing the outcrops of the Variscan basement in the Iberian Peninsula and subdivision of the Iberian Massif (taken from [Martínez Catalán et al., 2014](#)). Mafic igneous CALC (calc-alkaline), THOL (tholeiitic) and ALK (alkaline) outcropping areas are marked. Late Cadomian CALC-1 rocks are from the southern Central Iberian Zone (Carrascal and Mérida plutons; [Solá et al., 2003](#); [Bandrés et al., 2004](#)) and from the parautochthonous of the Morais Complex (Mora basalt, [Dias da Silva et al., 2014](#)). THOL-1 rocks are from the Segovia area ([Villaseca et al., 2015](#)). Pre-Variscan tholeiitic metabasites from northern Portugal, tentatively correlated with this event ([Cotrim et al., 2021](#)), are also indicated (with question marks). ALK-1 rocks are from the Almadén area ([Higueras et al., 2013](#)). THOL-2 outcrops are from La Codosera area ([López-Moro et al., 2007](#)). Tholeiites from the Almadén area are also situated (with question mark). Variscan CALC-2 gabbros are taken from [Orejana et al. \(2020\)](#) and [Bea et al. \(2021, and references therein\)](#). Monzonitic rocks from the Spanish Central System and the Sierra Bermeja pluton are from [Villaseca et al. \(2004\)](#) and [Errandonea \(2019\)](#), respectively. Permian ALK-2 dykes are from [Orejana et al. \(2008\)](#). Late Triassic Messejana-Plasencia tholeiitic dyke (THOL-3) is taken from [Cebriá et al. \(2003\)](#) whereas the Algarve area is from [Martins and Kerrich \(1998\)](#). Lusitanian alkaline rocks (ALK-3) are from [Mata et al. \(2015\)](#). Late Cretaceous alkaline massifs (Monchique, Sines and Sintra, ALK-4) are taken from [Grange et al. \(2010\)](#). Cenozoic Calatrava volcanic field (ALK-5 rocks) is taken from [Ancochea and Huertas \(2021\)](#). The Spanish Central System location, to the north of Madrid, is indicated. Inset is a sketch of the Variscan Belt in Western Europe showing the location of the most relevant Variscan terranes mentioned in text.

felsic plutonism ([Fig. 2](#)) and its subordinate associated subvolcanic rocks (the well known *Ollo de Sapo* formation) (e.g., [García-Arias et al., 2018](#)).

The first event of mafic magmatism without a significant felsic counterpart in the CIZ corresponds with small dykes, sills and laccoliths intruding into the peraluminous granitic Cambrian-Early Ordovician augen gneisses and the Neoproterozoic-Cambrian metasediments, in the Spanish Central System (THOL-1 in [Fig. 1](#)). These mafic rocks are mainly tholeiitic gabbroic metabasites, although subordinate fractionated types (leucotonalites) also appear ([Villaseca et al., 2015](#); [Orejana et al., 2017](#)). Two groups of metabasites were distinguished: those from the northern

Tenzuela massif, and those from the southwestern Revenga-El Caloco area. The first group has a HP-MT (eclogite/HP granulite) metamorphic imprint due to its deep burial during the Variscan collision ([Barbero and Villaseca, 2000](#)), whereas primary igneous features were preserved in the Revenga area. They yield ages of 473–453 Ma (in situ U–Pb zircon data) and the involvement of two different mantle lithospheric sources have been suggested due to their heterogeneous Sr–Nd isotopic composition ([Orejana et al., 2017](#)). Recently, pre-Variscan tholeiitic metabasic rocks have been described in central-north Portugal ([Fig. 1](#)) and have been correlated with these Tenzuela types for their similar

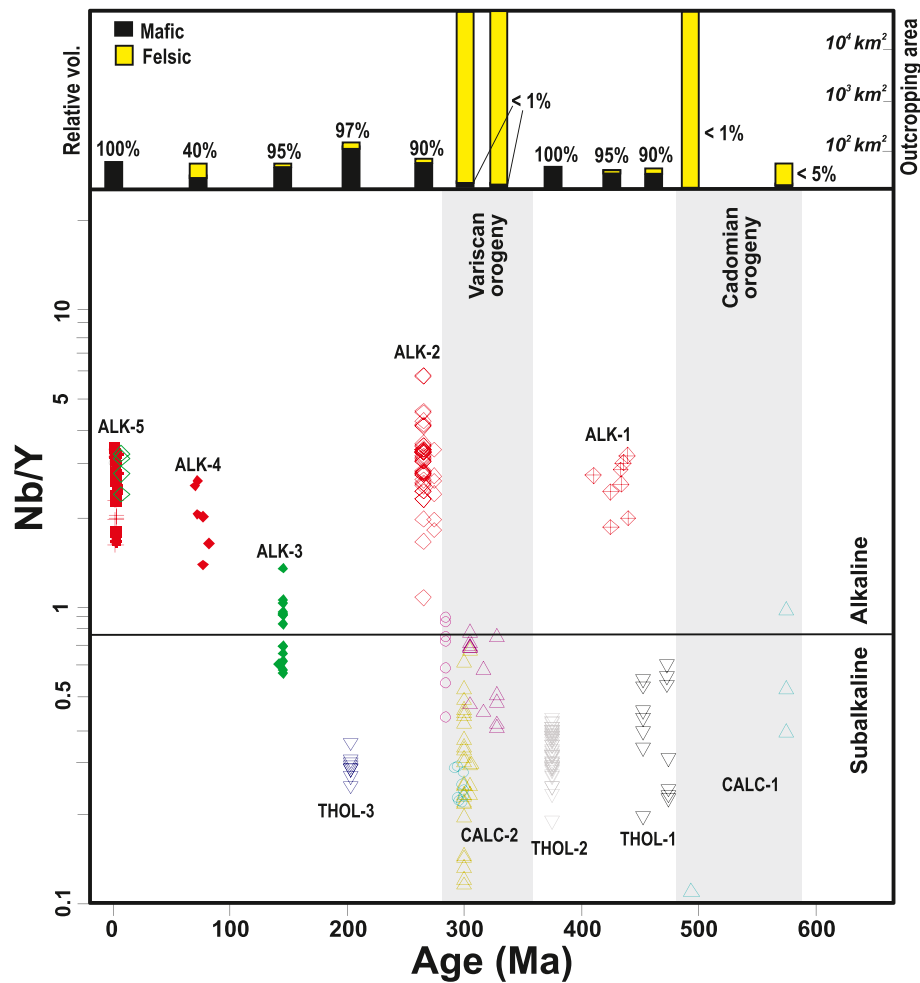


Fig. 2. Nb/Y vs. time (in Ma) comparing data of mafic rocks from the Central Iberian Zone (CIZ). Alkaline and subalkaline fields taken after [Pearce \(1996\)](#). Relative volumes of mafic (to felsic) types are estimated from literature for each magmatic cycle recorded in the CIZ (and expressed in vol% in each column). The outcropping area of the magmatic events is roughly estimated from cartography. CALC-2 symbols are detailed in caption to [Fig. 3](#).

geochemical (major, trace and Sr—Nd isotopes) features ([Cotrim et al., 2021](#)). Nevertheless, additional petrological and geochronological works are required to better constrain this event.

During this inter-orogenic period some interlayered Silurian and Devonian volcanic rocks of alkaline or tholeiitic affinity also appear (e. g., [Gutiérrez-Marco et al., 2019](#)). The more varied and abundant alkaline rocks outcrop in the Almadén area (ALK-1, [Fig. 1](#)), related with the gigantic Hg ore deposits ([Higueras et al., 2013](#)), although minor outcrops can also be found in central parts of Iberia (e.g., El Castillo, dated at 395 Ma by [Gutiérrez-Alonso et al., 2008](#)). Unfortunately, no significant geochemical and isotopic studies have been performed on these volcanics due to their great alteration. In the southwestern CIZ, a tholeiitic suite of sills and dykes intrusive into Late Devonian sequences has been described in the La Codosera area (THOL-2, [Fig. 1](#)), including major, trace and Nd isotopic data ([López-Moro et al., 2007](#)). Some other tholeiitic diabasic sills and dykes have also been described in the southern CIZ (e.g., THOL-2, near Almadén area, [Fig. 1](#)), although without detailed geochronological and geochemical studies, and consequently not included in this review.

During syn- to late stages of the Variscan collision voluminous granitic bodies from central to NW Iberia were generated. Scarce coeval mantle-derived magmas (CALC-2, [Fig. 1](#)) accompanied these felsic melts, giving rise to small gabbro and diorite intrusions and dyke swarms up to km in length ([Fig. 1](#)). The age range of 316–294 Ma obtained for the CIZ gabbros (U—Pb zircon data, e.g., [Días et al., 2002](#); [Orejana et al., 2020](#); [Bea et al., 2021](#) and references therein) are in

accordance with the ages determined on the coeval Variscan granites (e. g., [Orejana et al., 2012](#)). Microdioritic dyke swarms, accompanied by felsic granitic porphyries, crosscut some of those large granite batholiths giving similar ages (300 ± 1.4 Ma; Ar—Ar on amphibole; [Orejana et al., 2020](#)). The microdiorites are geochemically similar to the gabbroic-dioritic plutonic association, with fractionation and magma mixing as the main differentiation processes involved ([Huertas and Villaseca, 1994](#); [Orejana et al., 2009](#); [Scarrow et al., 2009](#)). The monzonitic calc-alkaline rocks include some of the first manifestation of Variscan mafic magmatism in the CIZ (328–316 Ma, [López-Moro et al., 2017](#); [Bea et al., 2021](#)), which are mainly biotite or amphibole-bearing monzogabbros (vaugnerites), outcropping almost exclusively in the NW Iberian Massif ([Fig. 1](#)). Similar magmatic events also appear in the southern CIZ (305 Ma, Sierra Bermeja, [Errandonea, 2019](#)) and in central Spain as the last Variscan calc-alkaline event (ca. 286 Ma; [Orejana et al., 2020](#)) ([Fig. 1](#)). This last magmatic event is represented by micro-monzonitic to microgabbroic dykes of shoshonitic affinity ([Orejana et al., 2020](#)) that outcrop within a restricted area of the Spanish Central System (Gb3 swarm in [Fig. 1](#) of [Villaseca et al., 2004](#)). All these Variscan mafic rocks (gabbros, microdiorites and monzonitic gabbros) display incompatible trace element contents characteristic of magmas from collisional orogens (e.g., negative Nb—Ta anomalies, high Th/Yb, low Ce/Pb; Supplementary Fig. S1).

A suite of volatile-rich mafic-ultramafic alkaline dykes (ALK-2) follows the Variscan calc-alkaline series. This group of thin N-S dykes, circumscribed to the Spanish Central System ([Fig. 1](#)), has been

Table 1

Main features of the Neoproterozoic to Cenozoic mafic rocks from the Central Iberian Zone.

Mafic episodes		Age (Ma)	Lithology	Geochemistry	Outcrop	Localities
This work	SCS types*					
CALC-1	Cadomian orogeny	580–570 486–471 494	Gabbros and hornblendites to granodiorites Gabbro to granodiorite Basalts	Subalkaline calc-alkaline suite (medium-high K)	Plutonic massif Plutonic massif Volcanic layers	Mérida (Cáceres) Carrascal Mora (Portugal)
THOL-1		473 473–453	Gabbroic metabasites	Subalkaline tholeiitic suite	Small intrusions in the SCS (sill-types)	Tenzuela (Segovia) Revenga, Caloco (Segovia) Porto (Portugal)?
ALK-1		ca. 440–380 395	Basanites to trachybasalts Basalts	Alkaline	Volcanic layers	Almadén (Ciudad Real) El Castillo (Salamanca)?
THOL-2		Post-late Devonian	Metabasites	Subalkaline tholeiitic suite	Sills and dykes	La Codosera (Badajoz) Almadén (Ciudad Real)?
CALC-2	Gb1	316–290	Gabbros (appinites)	Subalkaline calc-alkaline suite (medium to high K)	Small rounded intrusions coeval with granites	Small massifs dispersed over the CIZ (Portugal and Spain)
<i>Monzonites</i>	Gb2	300–292	Microgabbros-microdiorites (appinites)	Subalkaline calc-alkaline suite (medium-K)	E-W km-long swarm dykes coeval with granites	Spanish Central System
		328–316 305 (Monzon.1)	Gabbros and monzogabbros (vaugnerites)	Subalkaline calc-alkaline suite (shoshonitic)	Small intrusions Small bodies coeval with granites	Galicia - Domo Tormes Sierra Bermeja (Badajoz)
	Gb3	286	Microgabbros		NE-SW dykes coeval with granites	Spanish Central System
ALK-2	Gb4	274 271–264	Diabases Lamprophyres and monzo-syenites	Strongly alkaline suite	N-S dyke swarms	Spanish Central System
THOL-3	Gb5	203	Gabbros Basalts	Subalkaline tholeiitic suite	Great dyke: 50–100 m thick, 550 km length	Messejana-Plasencia dyke Minor volcanic deposits West Iberian margin (Lusitanian region)
ALK-3		148–140	Gabbros to diorites	Subalkaline to alkaline	Sills and dykes	SW Atlantic coast of Portugal
ALK-4		88–69	Gabbro to nepheline syenite	Alkaline	Mostly zoned intrusive complexes	
ALK-5		7.4 (K-rich event) 3.7–0.7 (Na-rich event)	Leucitites Melilitites, nephelinites and basalts	Ultralkaline	Lavas and piroclastic rocks	Calatrava volcanic field (central Spain)

* Following Villaseca et al. (2004) nomenclature, SCS = Spanish Central System.

subdivided into diabases and camptonitic lamprophyres to monzo-syenitic porphyries on the basis of petrographic and geochemical data (Orejana et al., 2008). Geochronological studies have provided Permian intrusion ages in the range 274–264 Ma (Orejana et al., 2020 and references therein).

After this alkaline event, a large tholeiitic dyke (Messejana-Plasencia) intruded the Iberian Peninsula near the Jurassic–Triassic transition (203 ± 2 Ma; Ar–Ar in biotite; Dunn et al., 1998) forming part of the Central Atlantic Magmatic Province (THOL-3, Fig. 1). Early Jurassic volcanic sequences from the Algarve (196.6 to 199.1 Ma after Ar–Ar dating; Verati et al., 2007) are also related to this province (e.g., Martins and Kerrich, 1998; Martins et al., 2008).

Finally, three successive alkaline cycles of sporadic intraplate magmatism intruded from western to central Iberia, which are mostly related to the ongoing opening of the Atlantic Ocean and post-rifting processes linked to plume-like structures rooted in sublithospheric central Atlantic anomalies (e.g., Civiero et al., 2021). The first stage is a minor event of moderately alkaline to slightly subalkaline magmatism at 148–140 Ma, registered in the western Iberian Margin (Grange et al., 2008; Mata et al., 2015) (ALK-3, Fig. 1). The second event is a Late Cretaceous (94–69 Ma) alkaline magmatism comprising more silica-undersaturated magmas than in the previous cycle, mostly outcropping as large zoned subvolcanic complexes along the SW Atlantic coast of Portugal (ALK-4, Fig. 1) (e.g., Bernard-Griffiths et al., 1997; Miranda et al., 2009; Grange et al., 2010) (Fig. 1). The third anorogenic magmatic event in the CIZ appears in central Iberia giving rise to the Cenozoic Calatrava volcanic field (ALK-5, Fig. 1) (7–0.7 Ma, Ancochea and

Huertas, 2021), spreading the incoming of OIB-type basalts with geochemical signatures related to the European Asthenospheric Reservoir (EAR) from Late Cretaceous to present. However, the presence of ultralkaline potassic magmas in this field (leucititic rocks of the Morrón de Villamayor volcano, MVM) suggests the involvement of an enriched lithospheric mantle component within the dominant asthenospheric sources of this intraplate Na-rich alkaline magmatism (e.g., Lustrino et al., 2019).

3. Samples and analytical methods

The whole-rock geochemical data of the mantle-derived rocks formed from Late Neoproterozoic to Pleistocene in the CIZ are shown in the Supplementary Table S1. This includes major and trace element contents of 230 whole-rock analyses of mafic rocks with MgO contents in excess of 4.0 wt% (Supplementary Table S1). Most data have been taken from the literature, of which 104 analyses (45% of the total amount) have been obtained by our research team. This contribution includes 21 unpublished analyses, four of them of metabasaltic samples from the Almadén area (ALK-1 rocks), in order to increase the previous scarce geochemical data on this alkaline event. The major and trace element whole-rock analyses were carried out at ACTLABS (Ontario, Canada). The samples were melted using LiBO_2 and dissolved with HNO_3 . Inductively coupled plasma atomic emission spectrometry (ICP–AES) was used for major element analysis, whereas trace elements were determined by inductively coupled plasma mass spectrometry (ICP–MS). Uncertainties in major elements range from 1 to 3%, except

for MnO (5–10%). The precision of ICP–MS analyses at low concentration levels has been evaluated from the repeated analyses of the international standards NIST-694, DNC-1, JR-1, W-2, SY-4 and BIR-1. The precision for trace elements is in the range 1–5%.

Supplementary Table S2 gathers the isotopic information on Sr–Nd–Pb systematics on the studied mafic suites. A total of 108 samples have been considered, 65 of them (60% of the sampling) correspond with new data or have been taken from previous studies by our research team (e.g., Villaseca et al., 2020; Orejana et al., 2020 and references therein). The Sr and Nd isotopic compositions of 10 new samples from Almadén, Variscan gabbros, Messegana-Plasencia and Calatrava (ALK-1, CALC-2, THOL-3 and ALK-5 rocks, respectively) were determined using a Phoenix-IsotopX Multicollector Thermal Ionization Mass Spectrometer with data acquired in multidynamic mode at the CAI of Geochronology and Isotope Geochemistry (Complutense University of Madrid, Spain). Repeated analyses on the NBS-987 standard (ref.value: 0.710248 ± 0.000003) gave $^{87}\text{Sr}/^{86}\text{Sr} = 0.710246 \pm 0.000013$ (2σ , $n = 16$) and values of $^{143}\text{Nd}/^{144}\text{Nd} = 0.512109 \pm 0.000005$ (2σ , $n = 14$) were obtained for the La Jolla standard (ref.value: 0.512115 ± 0.000002). The

2σ analytical errors are 0.01% for $^{87}\text{Sr}/^{86}\text{Sr}$ and 0.006% for $^{143}\text{Nd}/^{144}\text{Nd}$, which yield a 2σ error on ϵ_{Nd} calculation of ± 0.1 . Nd model ages have been calculated considering the following ratios for the Depleted Mantle: $^{147}\text{Sm}/^{144}\text{Nd} = 0.222$ and $^{143}\text{Nd}/^{144}\text{Nd} = 0.513114$ (Michard et al., 1985). The BHVO-2 standard was used as a quality control yielding analyzed mean values of $^{87}\text{Sr}/^{86}\text{Sr} = 0.703493 \pm 0.00005$ (2σ , $n = 81$) and $^{143}\text{Nd}/^{144}\text{Nd} = 0.513006 \pm 0.00005$ (2σ , $n = 81$) in agreement with the recommended values (Weis et al., 2006; Li et al., 2007).

Ten new Pb isotope analyses on samples from THOL-1, CALC-2 and ALK-5 groups (Supplementary Table S2) have been carried out at ACTLABS (Ontario, Canadá) following the method description of White et al. (2000). Samples were dissolved in a mixture of concentrated HF + HNO₃ mixed in the proportion 3:1 in Teflon vessels. Pb isotope ratios were measured on a MC-ICP-MS NEPTUNE (Thermo Fisher Scientific) mass spectrometer. Mass discrimination effect was corrected for reference $^{205}\text{Tl}/^{203}\text{Tl} = 2.3889$, which was measured in each mass spectrum (scan) strictly simultaneously with measurement of Pb isotope ratios. Analyzed Pb solutions were preliminarily spiked with standard Tl

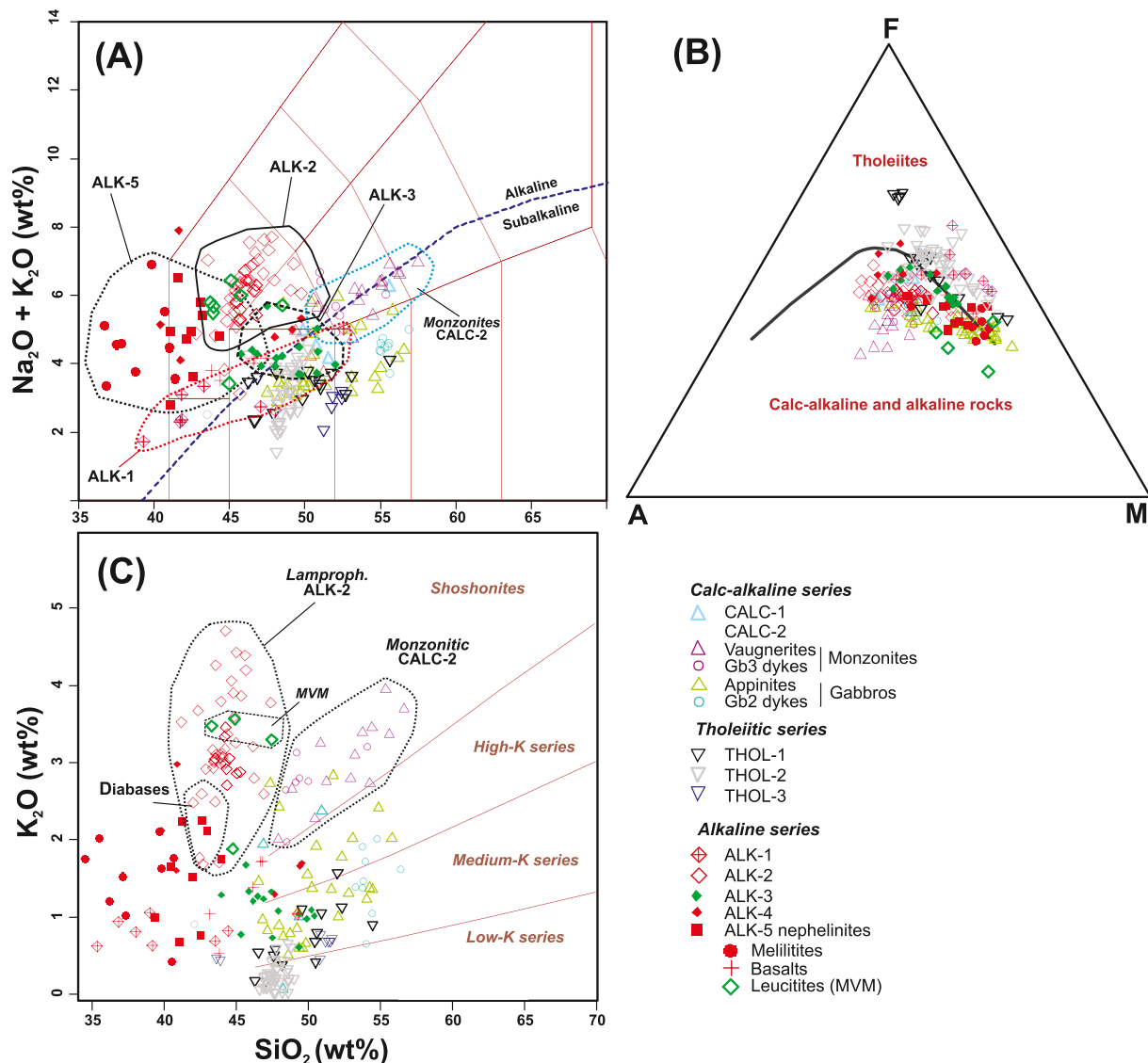


Fig. 3. Whole-rock major (in wt%) element composition of the mantle-derived rocks from the Central Iberian Zone: (A) Total alkalis vs. SiO₂, (B) AFM (A = Na₂O + K₂O, F = FeO_{total}, M = MgO) and (C) K₂O vs. SiO₂ diagrams. Classification fields taken from Rollinson (1993 and references therein). Monzonitic Gb3 and microgabbroic Gb2 dyke swarms from the Spanish Central System is the nomenclature from Villaseca et al. (2004). Some metabasaltic rocks from the Almadén area (ALK-1 rocks) plot in the tholeiitic field of the AFM diagram due to their low alkali content after hydrothermal alteration. MVM = Leucite rocks from the Morrón de Villamayor volcano (Calatrava volcanic field).

sample. The obtained Pb isotope ratios were corrected for instrumental fractionation from repeated measurement of Pb reference standard NBS 981. The measurement uncertainties in Pb isotope ratios in experiments ($\pm 2SD$) vary from 0.006 to 0.024%, being for most samples less than total analytical errors ($\pm 2SD$). The precision of results was controlled by the systematic analysis of NBS 981 standard displaying a good agreement with recommended values ($^{206}\text{Pb}/^{204}\text{Pb} = 16.93925 \pm 0.00058$, $^{207}\text{Pb}/^{204}\text{Pb} = 15.49663 \pm 0.00033$, $^{208}\text{Pb}/^{204}\text{Pb} = 36.71100 \pm 0.00098$) (e.g., Klaver et al., 2016). BHVO-2 standard was used for quality control giving comparable values with the reference material ($^{206}\text{Pb}/^{204}\text{Pb} = 18.6282 \pm 0.0004$) (Weis et al., 2006).

4. Insights from whole-rock geochemistry of mantle-derived magmas

4.1. Classification of magma series

The mafic rocks considered in this study define different chemical magmatic series (Table 1). Based on immobile trace element ratios (e.g., Nb/Y ratios, Fig. 2) along with the total alkalis versus silica (TAS) and AFM plots (Fig. 3) and on the petrographic descriptions from the literature, these rocks are classified in the calc-alkaline, tholeiitic and alkaline magmatic series, each one subdivided in several suites of different age:

(1) Calc-alkaline magmatic series intruded into the CIZ, during the Cadomian and Variscan orogenic cycles. The first one (CALC-1) is the oldest in this area and it is represented by the scarce intrusions that appear in boundary areas of the CIZ with either the Ossa-Morena Zone (OMZ) or the Galicia-Trás-os-Montes Zone (GTMZ). A scarce number of analyses are available, limited to mafic rocks from the gabbro-diorites of the Mérida massif (575 Ma; Bandrés et al., 2004) or from the Carrascal massif (c. 475 Ma; Solá et al., 2010), both located close to the boundary with the OMZ (Fig. 1). In these plutonic complexes, mafic rocks coexist with abundant felsic rocks, developing mixing features indicative of their coeval emplacement. Mafic types define a medium- to high-K magmatic suite of calc-alkaline affinity (Bandrés et al., 2004; Solá et al., 2010). The calc-alkaline Mora metabasalts of NE Portugal, within the parautochthonous of the GTMZ, are representative of the rare and scattered volcanic outcrops of Late Cambrian age (494 Ma; Dias da Silva et al., 2014) that appear in this northern sector, in the vicinity of the boundary with the CIZ. More abundant felsic rocks (andesite to rhyolite) are coeval with these basic terms.

The intrusion of these scarce and marginal bimodal mafic-felsic CALC-1 magmas is coeval with the generation of voluminous granitoid plutons in the innermost CIZ areas (with a minor input of rhyodacitic volcanics within the “Ollo de Sapo” formation). These later felsic intrusions define two plutonic belts, the largest being an array of highly peraluminous silica-rich metagranitic batholiths of metasedimentary derivation (e.g., Villaseca et al., 2016, and references therein). This is the first significant intracrustal recycling event recorded in the CIZ (Fig. 2).

The second calc-alkaline cycle (CALC-2) is related to the collisional Variscan orogeny and is compositionally more complex, intruding massively throughout the CIZ. The whole group of CALC-2 mafic magmas comprise two compositional end members (e.g., Bea et al., 2021). One is a high-K component that make these rocks to plot in alkaline or shoshonitic fields in the TAS and in the SiO_2 vs K_2O plots (Fig. 3), being called monzonitic (or vaugneritic) gabbros in the literature (e.g., López-Moro and López-Plaza, 2004; Gallastegui, 2005; Errandonea et al., 2018; Orejana et al., 2020). These monzonitic gabbros have remarkable higher LILE, LREE and Pb-Th-U contents (Supplementary Fig. S1) than the other Variscan gabbros (e.g., Bea et al., 2021). The second and most common mafic component of CALC-2 rocks in central Iberia is represented by subalkaline medium- to high-K calc-alkaline gabbros (also named appinites by some authors, see Bea et al., 2021 and references therein). Both suites overlap in their emplacement

ages, although the monzonitic types define a broader time span (328–286 Ma, from Bayo-Vigo vaugnerites to Gb3 monzonitic-shoshonitic dyke swarms) than the calc-alkaline gabbros (317–292 Ma, from Sanabria gabbros to Gb2 microdiorite dyke swarms) (Bea et al., 2021; Orejana et al., 2020). The abundant modal content of amphibole and/or biotite in both gabbro types (up to 36 vol%, Bea et al., 2021) is evidence for the H_2O -rich nature of these calc-alkaline mafic melts.

Similarly to the calc-alkaline late Cadomian cycle, the Variscan CALC-2 gabbros are accompanied by a huge volume of granitoids, leading to an overwhelming dominance of felsic rocks over an extremely minor input of mantle-derived magmas (< 1 vol%). The mafic rocks show a variable degree of mixing with coeval acid melts (e.g., Bea et al., 1999; Dias et al., 2002; Villaseca et al., 2011), although in this work we have been careful to deal only with the most primitive gabbros described in each massif. The huge volume of Variscan granitoids are the evidence of the second and most important intracrustal recycling event recorded in the CIZ (Fig. 2).

(2) Tholeiitic mafic magmas mostly appear scattered between the two main orogenic periods defined in the CIZ. At least three well-defined tholeiitic suites have been described. The first event (THOL-1) is represented by the Ordovician metabasites (473 to 453 Ma) outcropping in the Spanish Central System (Villaseca et al., 2015; Orejana et al., 2017). This mafic input is mainly composed of mafic lithologies (> 90 vol%), with subordinate felsic fractionates (leucotonalites) in the largest massif (Tenzuela). The metagabbros from this latter massif exhibit more radiogenic Nd isotope ratios, display lower LILE, LREE and Pb contents, and show higher Ti—Fe values compared with the rest of THOL-1 rocks (Orejana et al., 2017). These geochemical differences suggest the involvement of two contrasted mantle sources for this event.

A second tholeiitic magmatism (THOL-2) appears within Late Devonian metasedimentary sequences, close in time to the first stages of the Variscan collision. This THOL-2 cycle is not still accurately dated and its age has been constrained by its thermal imprint in stratigraphically fossiliferous Devonian metasedimentary sequences (Gutiérrez-Marco et al., 2019). The THOL-2 rocks display geochemical features similar to the Tenzuela metabasites (THOL-1), such as a negative K anomaly and the lack of Nb—Ta depletion in multitrace primitive mantle normalized patterns (Supplementary Fig. S1). Some sub-alkaline quartz-bearing diabases found near the alkaline rocks of the Almadén area (Fig. 1), intruding Devonian sequences, can be probably related to this tholeiitic event.

The third tholeiitic event (THOL-3) corresponds to the 550 km-long Messejana-Plasencia dyke that traverses the Iberian Peninsula from SW Portugal to central Spain (Fig. 1), intruding near the Triassic-Jurassic transition, during the opening of the central Atlantic Ocean. Some volcanic and volcanoclastic deposits interbedded in Late Triassic-Early Jurassic dolomitic limestones in the Algarve (south Portugal) are also related to this tholeiitic event (Fig. 1) (e.g., Martins and Kerrich, 1998; Martins et al., 2008; Callegaro et al., 2014). These tholeiites are similar to group-2 of the THOL-1 cycle for having a similar multitrace element pattern with Nb—Ta and P negative anomalies (Supplementary Fig. S1). Parental magmas of these continental tholeiites came from an enriched lithospheric mantle source (e.g., Cebriá et al., 2003; Martins et al., 2008).

(3) Alkaline mafic magmas intruded in upper crustal levels after the orogenic cycles and represent the main intraplate magmatism for the last 150 Ma in the western Iberian microplate (Fig. 2). The oldest alkaline event recorded in the CIZ (ALK-1) is the intraplate volcanism of the Almadén area, interlayered within Silurian-Devonian metasedimentary rocks (stratigraphically from 440 to 380 Ma) and connected to the huge mercury deposit of central Spain (Higueras et al., 2013). Scarce analytical data have been performed in those rocks and no accurate geochronological studies have been undertaken. Moreover, the high degree of alteration shown by the metabasaltic rocks (LOI is between 5.4 and 17.4 wt%, Supplementary Table S1) evidences the strong impact of

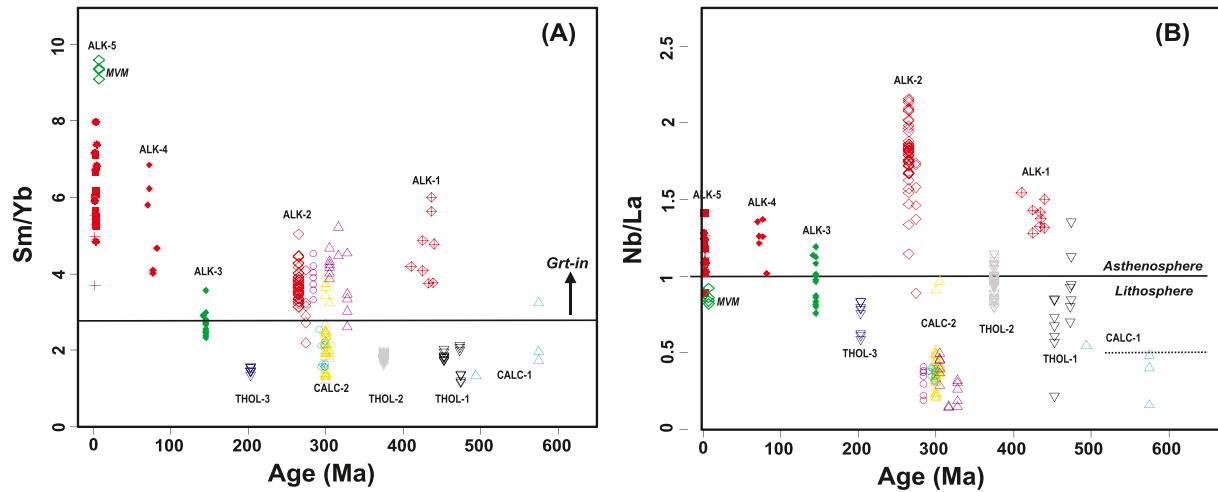


Fig. 4. Sm/Yb (A) and Nb/La (B) ratios vs. time (in Ma) of mafic rocks from the CIZ. Fields of garnet-bearing lherzolites and asthenospheric/lithospheric mantle sources are taken from Casetta et al. (2019) and references therein. Same symbols as in Fig. 3.

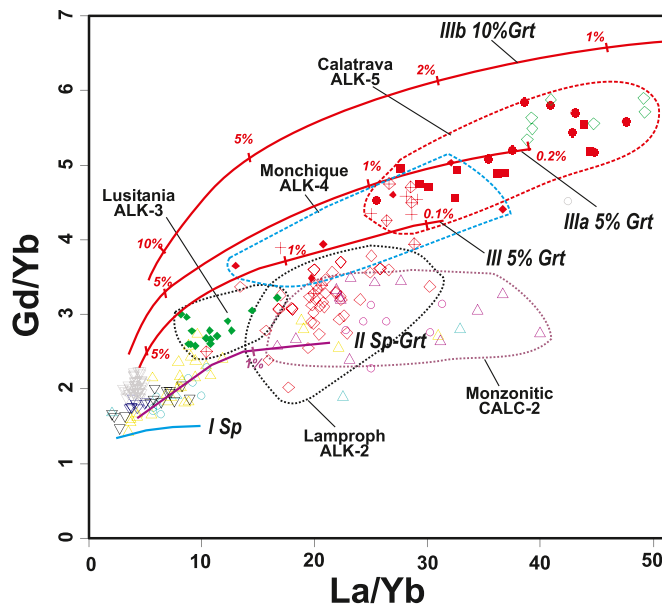


Fig. 5. Gd/Yb vs. La/Yb diagram with data of mafic rocks from the CIZ. Note that Almadén rocks (ALK-1) mainly plot within the ALK-4 field. Melting curves are calculated using the non-modal batch melting equation of Shaw (1970). Starting source is the fertile primitive mantle composition of Sun and McDonough (1989). Partition coefficients for minerals are from McKenzie and O'Nions (1991) and Schmidt et al. (1999) except REE for garnet in models IIIa and IIIb that are from Irving and Frey (1978). Curves I spinel peridotite (Ol57 + Opx28 + Cpx13 + Sp2), II spinel-garnet-amphibole lherzolite (Ol55 + Opx19 + Cpx15 + Sp2 + Grt4 + Amph5) and III garnet lherzolite (Ol55 + Opx25 + Cpx15 + Grt5) are from Casetta et al. (2019, their curves I, IV and III, respectively). Curves IIIa and IIIb are two garnet lherzolites (IIIa: Ol55 + Opx25 + Cpx15 + Grt5 and IIIb: Ol5 + Opx25 + Cpx15 + Grt10) with melting modes of Ol1 + Opx7 + Cpx60 + Grt32 in both cases. Number along lines represent the partial melting degree. Note that ALK-4 rocks (e.g., Monchique) plot between melting curves III of garnet lherzolites as ALK-5 rocks do, but at higher melt fractions. Same symbols as in Fig. 3.

hydrothermal metasomatism. Some major elements (e.g., Si, Fe, Na and K) and large ion lithophile (LILE) elements (e.g., Rb, Ba and Sr) have been leached making useless the major element characterization. High field strength elements (HFSE) and rare earth elements (REE) can be considered immobile during hydrothermal alteration (e.g., Pearce, 2014) and have been used for geochemical interpretation. This

magmatic cycle has been described as evolving from SiO₂-undersaturated ultrabasic-basic alkaline magmas to later transitional diabase dykes (Higueras et al., 2013). The high Nb/Y and La/Lu ratios of these alkaline rocks (e.g., Fig. 2) are similar to those shown by the other alkaline events of the CIZ. These ALK-1 magmas are low in K, plotting in transitional fields with subalkaline types in the TAS diagram (Fig. 3A). They plot in tholeiitic fields in the AFM diagram due to severe alkaline depletion during hydrothermal alteration (Fig. 3B).

The second alkaline event in the CIZ (ALK-2) occurred after the Variscan collision and comprises a group of northern-striking dyke swarms, mostly cross-cutting the Spanish Central System (Fig. 1). This dyke group is the K-richer suite of all the five alkaline cycles intruding in the CIZ along with the leucitic Morrón de Villamayor (MVM) volcano from the Calatrava field (Fig. 3C). These Permian ALK-2 rocks also have high Nb content, comparable with the Calatrava volcanic rocks (Fig. 2), but markedly low in Th, U and P contents (see marked Th, U and P negative anomalies in multi-trace patterns in Supplementary Fig. S1 when compared to ALK-5 rocks).

The third alkaline event (ALK-3) is a transitional suite registered in the Lusitanian area, to the north of Lisbon (Fig. 1). It comprises a few laccoliths and dykes, and no volcanic rocks have been reported (Mata et al., 2015). This event is chemically characterized for plotting in boundary fields with subalkaline types in the TAS diagram (Fig. 3A) and in trace element plots (e.g., Fig. 2), due to their low Nb contents compared to the other CIZ alkaline cycles. The ALK-3 rocks also stand out for being the alkaline group with flatter REE chondrite-normalized patterns (the lowest La/Lu, Gd/Lu and Sm/Yb ratios, e.g., Fig. 4A) and the lowest total REE contents (see also Supplementary Fig. S1).

The fourth alkaline event (ALK-4), also outcropping in western Portugal (Fig. 1), comprises plutonic massifs (up to 60 km², Monchique laccolith complex), isolated sills and plugs and a volcanic complex in the Lisbon area (e.g., Miranda et al., 2009; Grange et al., 2010). This event is characterized by the abundance of fractionated felsic rocks (syenites, granites), dominant over mafic types in the biggest massifs (Fig. 2). The mafic ALK-4 rocks are chemically similar to Na-rich volcanics of the ALK-5 Calatrava types, although exhibiting lower LREE contents and, consequently, less fractionated REE patterns (e.g., Fig. 4A). They show slight Pb, K and Zr—Hf negative anomalies in multi-element patterns, whereas displaying high Rb, Ba, Th, U and Nb contents (Supplementary Fig. S1), as is common in Cenozoic alkaline volcanic rocks from western Europe (e.g., Brandl et al., 2015; Pfänder et al., 2018).

The last magmatic activity in central Iberia corresponds with the Cenozoic alkaline intraplate Calatrava volcanic field (Fig. 1). This monogenetic volcanic field is mainly represented by Na-rich silica-

undersaturated mafic rocks (melilitites, nephelinites and basanites), although the oldest eruption (7.2 Ma) corresponds to the only K-rich volcano in the field (e.g., [Ancochea and Huertas, 2021](#)) (Fig. 3C). These volcanic ALK-5 rocks stand out for displaying the highest REE fractionated patterns among all the studied alkaline suites (Figs. 4, 5). The Calatrava Na-rich magmas are similar in composition to the ALK-4 mafic rocks, although showing higher LILE and LREE contents (Supplementary Fig. S1). The K-rich leucititic MVM volcano is also singular for its high Cs, Rb, Th, U and Pb contents (all of them >500 times primitive mantle values -PM- of [Sun and McDonough, 1989](#)), chemical features similar to typical upper crustal rocks or pelagic sediments ([Lustrino et al., 2019](#)). Although these MVM rocks are leucite-bearing basanites *sensu stricto* (Fig. 3A), instead of true leucitites (see discussion in [Lustrino et al., 2019](#)), both terms have been used indistinctly in the literature on this volcano.

4.2. Approaches to depth of melting and melt fraction

The knowledge of the subcontinental mantle section beneath a crustal block is essential to undertake any attempt on discussing depth of magma generation. Although the crust and lithospheric mantle beneath central Iberia have experienced a protracted evolution from the Neoproterozoic, associated to fairly different geotectonic settings, the current lithosphere has a variable thickness from 80 to 90 (under NW Iberia and the Calatrava Volcanic Field) to 110 km in most other areas of the CIZ (e.g., [Granja et al., 2015](#); [Palomeras et al., 2021](#)). According to these authors, the crust presents a normal thickness of about 31–35 km. Considering that the spinel-garnet transition may occur from 50 to 85 km, depending on the mantle composition (e.g., [Klemme and O'Neill, 2000](#)), and that a strong lithospheric thickening occurred during the Variscan collision, spinel-garnet- and garnet-bearing lherzolites might have been common in the deepest subcontinental lithospheric mantle beneath central-western Iberia from Late Paleozoic times.

Most of the recorded mafic rocks lack characteristics of primary melts derived from mantle sources. They have low Cr (<1000 ppm) and Ni (<400 ppm) contents and their Mg# [(MgO)/(MgO + FeO)mol%] values do not reach 0.7, although some Variscan gabbros and Calatrava volcanics are close to these figures (Supplementary Table S1). Nevertheless, the use of incompatible trace element ratios from the most primitive samples (MgO > 4 wt%), which are less likely to have undergone significant magma fractionation, can be helpful when trying to constrain the partial melting conditions and the nature of the sources, as discussed below. This MgO value has been used in other petrogenetic studies to select primitive magmas to characterize chemical features of mantle sources (e.g., [Peccherillo, 2017](#)). In addition, only those trace elements considered immobile under low grade of metamorphism and hydrothermal processes ([Rollinson, 1993](#)) have been used to characterize pre-Variscan mafic rocks (e.g., ALK-1 rocks from the Almadén area). These geochemical fingerprints, together with the initial isotopic signatures, are reliable data to describe the chemical evolution of the mantle-derived rocks of central Iberia from the Neoproterozoic onwards, and to discuss their petrogenetic implications and its linkage with the geodynamic evolution of the upper mantle in this sector.

The depth of melt extraction can be estimated qualitatively studying the REE characteristics of the different suites, as this trace element group is very sensitive to the presence of garnet in lherzolite mineral assemblages and no significant modification of the REE ratios is expected as a consequence of possible crystal fractionation processes involving olivine, plagioclase or clinopyroxene. All ratios indicating REE fractionation (e.g., Sm/Yb, Gd/Yb or La/Yb) are higher in the alkaline rocks intrusive in the CIZ (Figs. 4 and 5). In fact, most alkaline rocks show affinity with an asthenospheric mantle when considering the Nb/La vs. La/Yb discrimination diagram, excepting part of the Lusitanian rocks (ALK-3 suite), which falls in the lithospheric area (Fig. 4B). The leucititic (K-rich) samples of the Calatrava field (MVM volcano of ALK-5 rocks) also plot in the lithospheric fields of those diagrams even having some of

the highest HREE fractionation (Fig. 4B). Likewise, the CIZ calc-alkaline rocks and most of the tholeiitic series (with the exception of some samples from THOL-1 and 2 cycles) plot in the lithospheric field. Nevertheless, if only HREE are considered some high-K (monzonitic or vaugneritic) mafic rocks of the Variscan cycle (CALC-2 series) show relatively high Sm/Yb ratios overlapping values of some alkaline series (Fig. 4A), suggesting their derivation from spinel-garnet-bearing mantle sources, as stated in previous works ([Orejana et al., 2020](#)). These results are coherent with the Iberian lithospheric section described above.

The covariation between La/Yb and Gd/Yb ratios cannot be only used to estimate garnet- or spinel-bearing lherzolite sources but also the degree of partial melting (e.g., [Casetta et al., 2019](#)). Although we know that estimates of partial melting degree depend largely on the composition of the source, we have used the same mantle protolith in all models of Fig. 5 in order to obtain comparative values. The Gd/Yb ratios of the alkaline suites fit better with the melting curves of garnet-bearing sources, although some of them might also involve hydrous phases (e.g., amphibole for Variscan gabbros; Fig. 5). Moreover, the highest La/Yb values of the Calatrava ALK-5 rocks among the alkaline suites are likely indicative of their derivation by partial melting at the lowest melting fractions of the studied mafic rocks, mostly below 2% melting of garnet-lherzolites, with a fertile primordial mantle (PM) source composition (Fig. 5), as also suggested by [Lierenfeld and Mattsson \(2015\)](#). On the contrary, most calc-alkaline and tholeiitic series show low Gd/Yb and La/Yb ratios indicating their derivation from spinel-bearing lherzolite lithospheric sources and higher degrees of partial melting (e.g., in the range of 10–35%; [Cebriá et al., 2003](#) and [López-Moro et al., 2007](#)). The K-rich Variscan gabbros (monzonitic types of CALC-2) display high La/Yb and Gd/Yb values, suggesting their derivation from garnet-bearing peridotites, most probably from the base of a thick lithospheric mantle ([Orejana et al., 2020](#)). Lithospheric mantle sources have been proposed for the origin of most Variscan mafic melts (e.g., [Dias et al., 2002](#); [Villaseca et al., 2004](#); [Orejana et al., 2009](#); [Bea et al., 2021](#)) although some parameters evaluated here (degree and depth of melting) are still poorly constrained.

Mafic lavas such as melilitites and nephelinites, with high incompatible trace element contents and strong REE fractionation in normalized plots, can represent primitive magmas derived from low degrees of partial melting of carbonate-rich mantle sources (e.g., [Foley et al., 2012](#); [Foley and Fisher, 2017](#); [Baudouin and Parat, 2020](#)). These silica-undersaturated magmas are common in the Calatrava Volcanic Field (ALK-5 rocks) and show some high trace element ratios typical of magmas derived from a CO₂-bearing lherzolite: Ce/Y > 5 and Zr/Hf > 45 (Supplementary Fig. S2) (e.g., [Dupuy et al., 1992](#); [Baudouin and Parat, 2020](#)). The presence of carbonate in the source, in combination with accessory hydrous minerals (e.g., phlogopite; [Cebriá and López Ruiz, 1995](#)) allows low melt volumes to be extracted from the mantle (e.g., [Stagno et al., 2018](#)). The common occurrence of hydrous metasomatic minerals and carbonatite imprints in lherzolite xenoliths transported by these alkaline magmas (e.g., [Villaseca et al., 2019](#)) agrees with the presence of volatile-rich mantle heterogeneities in the upper mantle beneath central Spain.

4.3. Mantle sources

Uncontaminated intraplate mafic magmas plot in the Th/Yb vs. Ta/Yb diagram within a band with a slope of unity, as mantle enrichment events concentrate Ta and Th equally ([Pearce, 1982](#)). Most of the CIZ mafic suites display enrichment in incompatible elements and moderate to high Th/Yb and Ta/Yb values that clearly differ from those typical of mid-ocean ridge basalts (MORB) (Fig. 6A), pointing to derivation from variable enriched mantle sources. The CIZ alkaline suites plot around the OIB composition, whereas tholeiites show a lower enrichment degree (Fig. 6A). Moreover, some tholeiitic suites, those appearing after orogenic events (THOL-1 and THOL-3), show a significant influence of subduction-related (crustal) components, reflected in their higher Th/

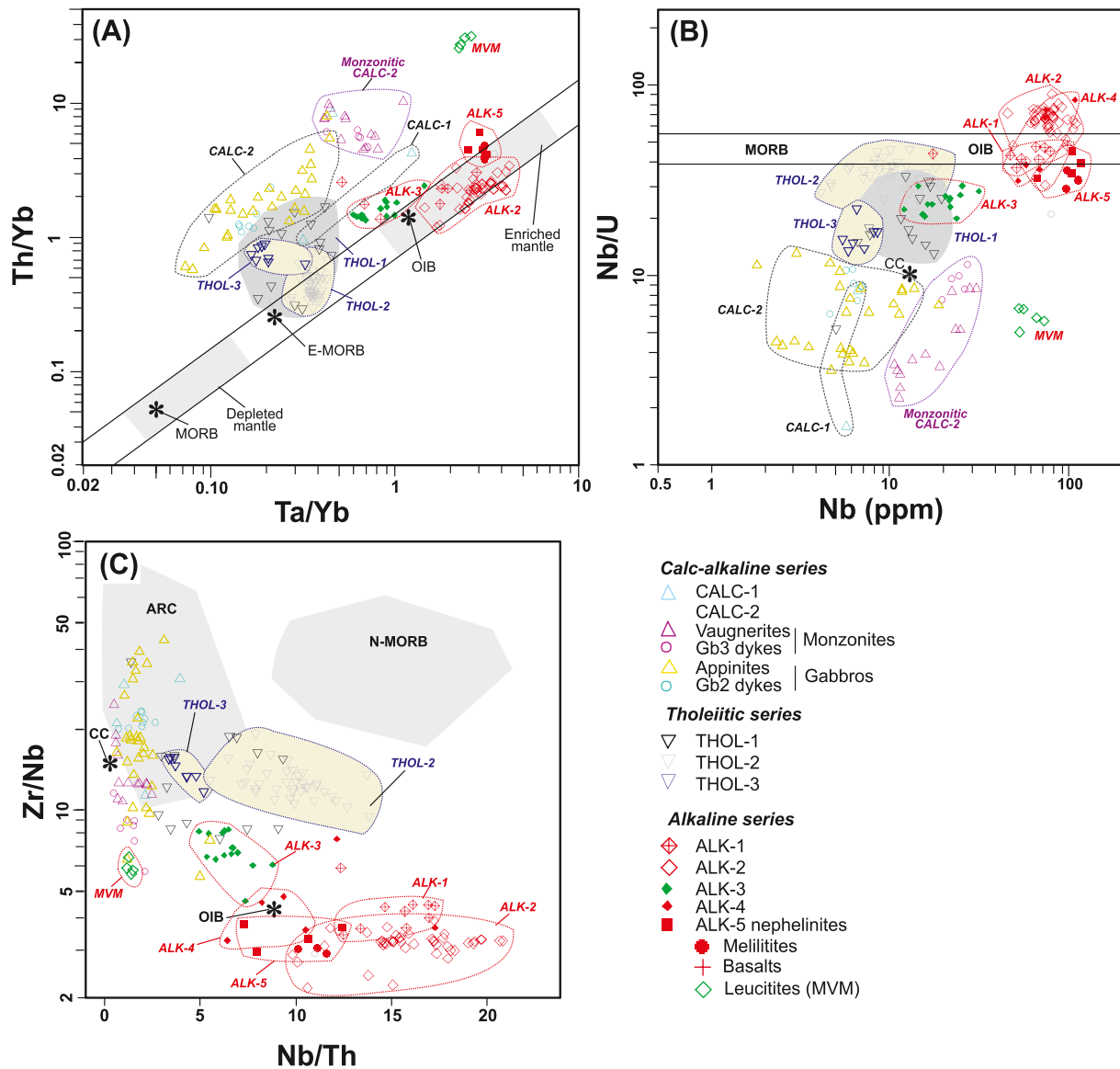


Fig. 6. Whole-rock trace element composition of the mafic rocks from the CIZ: (A) Th/Yb vs. Ta/Yb. Data for fields of MORB, E-MORB, OIB are after Sun and McDonough, 1989. Note that ALK-4 rocks are not shown due to the lack of Ta data (Supplementary Table S1) and ALK-1 rocks plot within ALK-2 and ALK-3 fields. (B) Nb/U vs. Nb. MORB and OIB values after Hofmann, 1997. Most alkaline suites (except ALK-3 rocks) overlap in the plot. Averaged Continental Crust (CC) after Rudnick and Gao, 2005. (C) Zr/Nb vs. Nb/Th. Fields for ARC, N-MORB, CC and OIB are from Condie, 2005. Most calc-alkaline rocks plot over the ARC (arc-related basalts) field.

Yb values, plotting close to the field of Variscan calc-alkaline gabbros (Fig. 6A). The monzonitic calc-alkaline rocks (vaugneritic gabbros and monzonitic dykes) also plot in subduction-related fields, but at higher Ta/Yb values than the rest of calc-alkaline rocks, suggesting a more enriched source. In this diagram, the leucititic rocks from the MVM volcano plot apart from Na-rich ALK-5 rocks, reaching the highest Th/Yb ratios of the whole dataset, also with high Ta/Yb values (Fig. 6A). Their plotting far away from OIB values suggest a significant crustally enriched lithospheric mantle component.

Most diagrams involving incompatible trace element ratios (Fig. 6) show that monzonitic calc-alkaline types (e.g., vaugnerites from CALC-2 series) and leucititic rocks (MVM rocks from ALK-5 series) plot close to the continental crust field because they have high Th, U and Pb contents. According to the major and trace element composition of the CIZ mafic rocks, heterogeneous and complex mantle sources were involved in these magmatic events over such an extended period.

The initial Sr–Nd isotopic composition of the CIZ mafic rocks is presented in Fig. 7A. Most alkaline rocks (ALK-2, -3, -4 and -5) plot in

the upper left quadrant, close to PREMA and HIMU reservoirs (Zindler and Hart, 1986). The whole data set defines a rough curvilinear array from these alkaline fields towards more radiogenic Sr isotope compositions, mostly defined by calc-alkaline Variscan gabbros (CALC-2 series), approaching the Iberian continental crust compositional field (Fig. 7A). The monzonitic types, which outcrop within the innermost CIZ (Monzon. 2 in Fig. 7A), display the highest radiogenic Sr values of this CALC-2 field suggesting some kind of crustal delamination or convective mantle flow bringing enriched components during different stages of the Variscan collision, as these mafic magmas come from deep lithospheric mantle sources (spinel-garnet bearing transition). On the contrary, monzonitic rocks from the Sierra Bermeja pluton (Monzon.1, Fig. 7A) might be derived from OMZ juvenile mantle levels underthrust below the CIZ during the Variscan collision due to its marginal position towards that boundary (Fig. 1). The tholeiitic rocks plot slightly outside this array, towards relatively enriched radiogenic Sr values alike those of the Silurian alkaline rocks of the Almadén area (ALK-1, Fig. 7A), considerably affected by hydrothermal alteration (Higueras et al.,

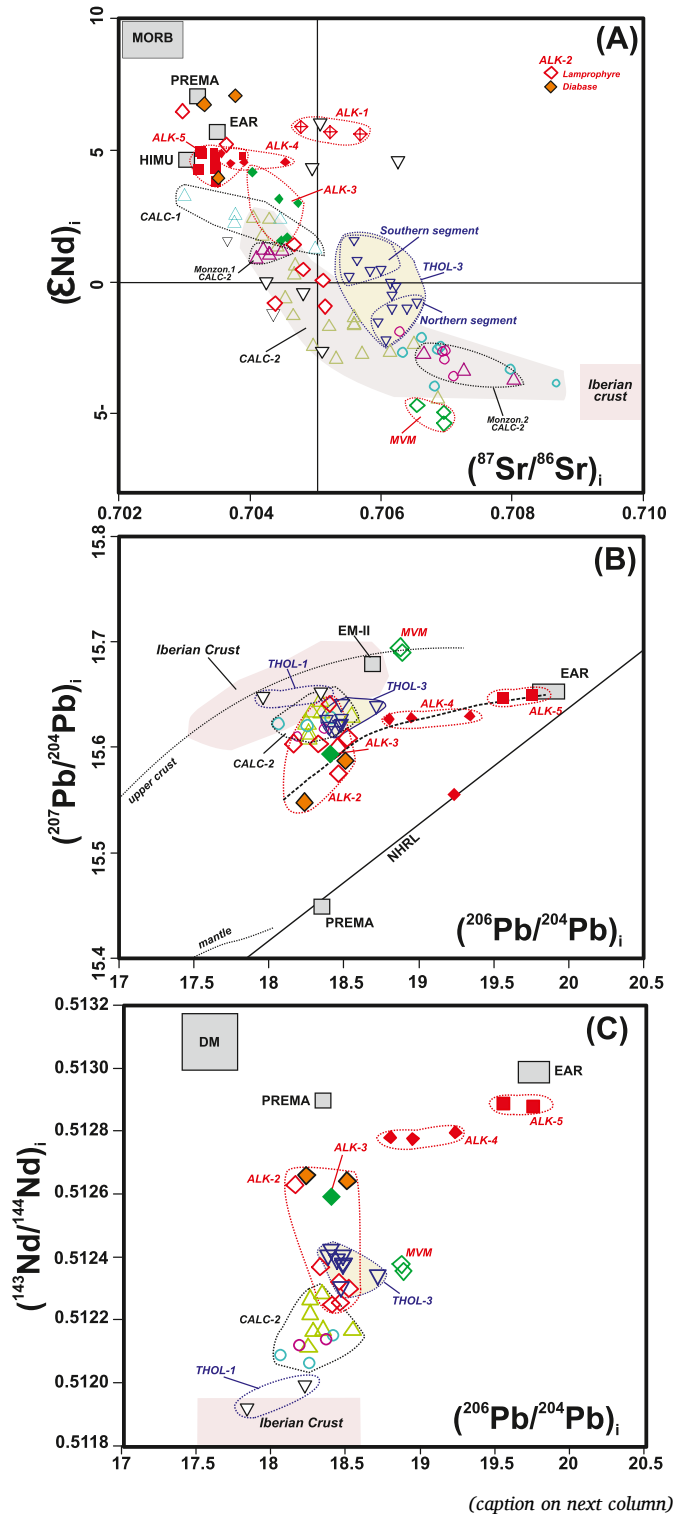


Fig. 7. Initial Sr-Nd-Pb isotope compositions of CIZ mafic rocks (A) ϵ_{Nd} vs. $^{87}\text{Sr}/^{86}\text{Sr}$ diagram. Monzon.1 and Monzon.2 refers to vaugnerites from Sierra Bermeja pluton and other outcrops (Vigo, Tormes Dome, Gb3 dykes), respectively. Composition of southern and northern segments of the great Messejana-Plasencia THOL-3 dyke are highlighted. (B) $^{207}\text{Pb}/^{204}\text{Pb}$ vs. $^{206}\text{Pb}/^{204}\text{Pb}$. NHRL reference line is from Rollinson, 1993. Upper crust and mantle evolution lines are from Zartman and Doe, 1981. (C) $^{143}\text{Nd}/^{144}\text{Nd}$ vs. $^{206}\text{Pb}/^{204}\text{Pb}$. Fields of MORB (Mid Ocean Ridge Basalt), DM (Depleted Mantle), PREMA (Prevalent Mantle Reservoir), EM-II (Enriched Mantle with high $^{87}\text{Sr}/^{86}\text{Sr}$), HIMU (High- μ Mantle, Pb enriched) and BSE (Bulk Silicate Earth) are from Rollinson, 1993. EAR (European Asthenospheric Reservoir) values after Cebriá and Wilson, 1995. Field for the Central Iberian continental crust (Iberian crust) is extrapolated from metamorphic and granitoid data from Villaseca et al., 1999, 2009 and Merino Martínez et al., 2014. Take note that HIMU values plot out of diagrams (B) and (C) due to their high Pb ratios ($^{206}\text{Pb}/^{204}\text{Pb}$ up to 21.69 and $^{207}\text{Pb}/^{204}\text{Pb}$ up to 15.84). In most diagrams, leucititic rocks from the MVM volcano (green diamonds) plot away from the ALK-5 field. Isotopic data taken from Supplementary Table S2 (and references therein). Same symbols as in Fig. 6. (For interpretation of the references to colour in this figure legend, the reader is referred to the web version of this article.)

2013). This effect is also evident in the case of the Ordovician metabasites (Tenzuela rocks of THOL-1 series, Supplementary Table S2) interpreted as due to metamorphism (Orejana et al., 2017). On the contrary, the Late Triassic Messejana-Plasencia dyke (THOL-3 rocks) has Sr–Nd values close to the present day BSE mantle component, suggesting the involvement of an enriched lithospheric mantle source (Cebriá et al., 2003; Callegaro et al., 2014). However, the isotopic heterogeneity of this large dyke, with more primitive values in the southwestern segment, has been associated to an increasing degree of lower crustal contamination towards the northeast (Cebriá et al., 2003). Moreover, the high radiogenic Sr isotope values of the leucititic MVM rocks is remarkable, indicating a markedly different mantle source when compared to the rest of ALK-5 series of the Calatrava field, probably due to metasomatism by crustal or lithospheric mantle components (e.g., Cebriá and López Ruiz, 1995; Lustrino et al., 2019).

The initial lead isotope composition of the studied mafic rocks (Fig. 7B) define a curvilinear trend for the alkaline series (ALK-2, –3, –4 and –5) and more scattered data for mafic magmas with crust-like values (calc-alkaline and tholeiitic series, including leucititic rocks from the MVM volcano of the ALK-5 event).

The combination of different isotopic systems indicates the involvement of at least three different mantle components for the alkaline series. First, a component with highly unradiogenic Sr, low $^{206}\text{Pb}/^{204}\text{Pb}$ and radiogenic Nd isotope ratios close to the PREMA reservoir (instead of a depleted mantle -DM- component), mostly defined by the Late Permian diabases (ALK-2 series, Fig. 7C). A second pole is a component with relatively radiogenic $^{206}\text{Pb}/^{204}\text{Pb}$ and Nd, and unradiogenic Sr isotope ratios, similar to the EAR mantle reservoir, very common in the Cenozoic magmatism of central Atlantic archipelagos and in the circum-Mediterranean area (Lustrino and Wilson, 2007). This component characterizes the Mesozoic to Cenozoic alkaline cycles in the Iberian Peninsula (some ALK-3 rocks and most of the ALK-4 and ALK-5 series). The third component, well illustrated by the Late Miocene leucititic rocks of the MVM volcano, shows high radiogenic Sr and unradiogenic Nd signatures, accompanied by relatively unradiogenic $^{206}\text{Pb}/^{204}\text{Pb}$ values, which has been identified as a lithospheric crustal component in the Western Mediterranean lamproites (e.g., Prelevic et al., 2008; Lustrino et al., 2019).

The scarce Sr-Nd-Pb isotopic data from CIZ mafic rocks of calc-alkaline and tholeiitic composition indicate the involvement of other two mantle sources. The first mantle component is characterized by highly radiogenic Sr and unradiogenic $^{206}\text{Pb}/^{204}\text{Pb}$ and Nd isotope ratios close to or overlapping Variscan granitoids and other crustal rocks of the CIZ (Fig. 7). The second pole is a mantle with Sr-Nd-Pb isotopic ratios similar to the composition of the Bulk Earth or a Primitive Mantle, if such a mantle reservoir still survives (Rollinson, 1993). Moreover, the

oldest mafic suites (CALC-1 and Tenzuela rocks of the THOL-1 series in Fig. 7A) display the more depleted mantle compositions. Exceptionally, Variscan vaugnerites from the southernmost CIZ (Monzon.2 CALC-2, the Sierra Bermeja pluton) show also slightly radiogenic Nd isotope ratios (Fig. 7A) and the lowest Nd model ages within the Variscan data (Supplementary Table S2). As stated above, their origin could be related to the melting of juvenile mantle sources derived from the thrusting, obduction and associated subduction of proto-oceanic domains from the Ossa Morena and South Portuguese Zones beneath the southern continental CIZ, from the Late Mississippian onwards (e.g., Ribeiro et al., 2010; Pérez-Cáceres et al., 2015).

5. Discussion

5.1. Geodynamic evolution and crust-mantle interaction under Central Iberia

All the Iberian pre-Variscan terranes have been considered as part of the northern, Andean-type continental margin of Gondwana during the Neoproterozoic to Cambrian, with subduction of the Iapetus and Tornquist Oceans from 800 to ca. 540 Ma, with a peak of magmatic activity of calc-alkaline magmas at 640–540 Ma (Cadomian orogeny, e.g., Stampfli et al., 2013 and references therein). This oceanic subduction evolved gradually and diachronously to a rifting or a passive margin environment during the Early Paleozoic, depending on the location of each peri-Gondwanan terrane along this large continental margin (Fig. 8). In this context, the Late Neoproterozoic–Early Ordovician calc-alkaline intrusions (CALC-1) can be considered late magmatic manifestations in the framework of the Cadomian cycle. The geochronology and geochemistry features of the older Mérida Massif are coherent with a classic oceanic subduction scheme, but the younger Early Ordovician rocks of the Carrascal Massif are likely associated with transition to an extensional scenario (Solá et al., 2010). In contrast, a flat subduction model developing crustal thickening of the innermost continental terranes has been proposed for the formation of the abundant peraluminous felsic magmas in the CIZ during the Cambrian–Early Ordovician transition (Villaseca et al., 2016). A subsequent passive margin would have developed, leading to deposition of a thick siliciclastic (mainly quartzitic) sedimentation of Floian age. The incoming of intraplate tholeiitic mafic magmas (THOL-1 series) is also coherent with this evolution towards a passive margin scenario in central Iberia (Orejana et al., 2017, 2020).

The scarce calc-alkaline metagabbros (CALC-1) and the first tholeiitic event (THOL-1) are mafic melts derived from shallow lithospheric mantle sources since their REE ratios are poorly fractionated (e.g., Figs. 4A and 5B). Their initial Sr–Nd ratios are also broadly in the same range, which would indicate derivation from similar enriched mantle sources, although the northern THOL-1 massif (Tenzuela area) points to the involvement of a more depleted component (Fig. 9). The low Th/Yb ratios of rocks from this massif plot in the mantle array and resemble E-MORB geochemical signatures (Villaseca et al., 2015), whereas the rest of THOL-1 rocks have higher Th/Yb ratios (Fig. 6A). The southern rocks from the THOL-1 suites also exhibit a tendency towards higher LILE contents and display negative Nb–Ta anomalies (Supplementary Fig. S1) and unradiogenic Nd values (Fig. 7A and Supplementary Table S2), likely associated with subduction of crustal components into the lithospheric mantle during the long-lasting Cadomian orogeny (Orejana et al., 2017). The absence of magmas originated from deeper mantle sources at that time could be related with the replacement of most of the deep subcontinental mantle by cold oceanic lithosphere during flat subduction (e.g., Axen et al., 2018).

The Silurian–Devonian alkaline to subalkaline volcanism of the CIZ (the Almadén area, ALK-1 series) involves the incoming of mafic melts from deep garnet-bearing mantle levels, as suggested by the high La/Yb, Sm/Yb or Gd/Yb ratios of the more silica-undersaturated alkaline rocks (Figs. 4A and 5B). Moreover, their high Nb contents (also Nb/U and Nb/Th ratios) suggest that OIB sources with the imprint of deep-seated

metasomatic agents, similar to those argued for later alkaline series, were involved in their formation. This agrees with the radiogenic Nd isotope ratios (average ϵ_{Nd} value of +5.6) and the young Nd model ages of these rocks, in the range of 589–627 Ma (Fig. 10 and Supplementary Table S2).

The intrusion of tholeiitic dykes in the southwestern CIZ (THOL-2 series) is coeval with the Early Variscan convergence in adjacent terranes (GTMZ), interpreted as originated mainly by oceanic accretion and the first stages of continental subduction in marginal microplates close to the CIZ (e.g., Ballèvre et al., 2014). During Late Devonian, the southernmost CIZ evolved from a passive margin scenario to an oblique convergence with the Ossa Morena and South-Portuguese Zones (Pérez-Cáceres et al., 2016). These other peri-Gondwanan terranes were probably located at westward latitudes, as they have different Paleozoic lithostratigraphic sequences when compared to the CIZ and because such paleogeographic configuration would resolve the left-lateral displacement described for those southern terranes assembled during the Variscan collision (e.g., Roubardet and Gutiérrez-Marco, 2002; Pérez-Cáceres et al., 2016) (Fig. 8). The Devonian intrusion (ca. 375 Ma; Gutiérrez-Marco et al., 2019) of tholeiitic sills and sheets in the CIZ edge (Fig. 1) was the last magmatic event before the onset of the Variscan collision in this terrane. This THOL-2 magmatism differs from the rest of tholeiitic suites in displaying a narrow range of moderately high initial ϵ_{Nd} values (from +5.4 to +5.8) and younger model ages ($T_{\text{DM}} = 735\text{--}620$ Ma) (López-Moro et al., 2007). This suggests the involvement of juvenile mantle sources more enriched than depleted or MORB mantle (Fig. 10) with no sign of significant continental crustal imprint, as shown by the low Th/Yb (Fig. 6A) and relatively high Nb/U (mostly from 20 to 47) values (Fig. 6B and Supplementary Table S1). The lack of supra-subduction signatures in THOL-2 rocks is in agreement with a Devonian within-plate scenario, such as a continental passive margin at the southern CIZ boundary (Fig. 8B).

The Variscan collision changed drastically the kind of lithospheric mantle sources involved, as subducted continental material becomes significant. This is most evident in the case of the K-rich CALC-2 igneous rocks. Some of the monzonitic gabbros of the CALC-2 cycle appear relatively late, after significant exhumation of the largely thickened crust has occurred, and coevally with abundant granitic magmatism, whereas the NW Iberia vaugnerites intruded after the nappe stacking of the GTMZ allochthonous terranes (Fig. 1). The K-rich gabbroid rocks are usually generated as low degree melts at deep lithospheric mantle sources (within the garnet stability field, Fig. 5), during late post-collisional stages (e.g., Dewey, 1988). Their high Ce/Nb ratios and almost constant low Nb/Th values suggest the presence of amphibole as the main hydrous mineral in the lithospheric mantle source (Orejana et al., 2020) (Supplementary Fig. S3). Moreover, most monzonitic rocks plot close to the Iberian continental crust field in some isotopic diagrams (e.g., Fig. 7A, C), indicative of the high crustal imprint in these mafic magmas. The relative abundance of alkali-feldspar and quartz ocelli (xenocrysts) and the lack of olivine (and scarce clinopyroxene) in most monzonitic CALC-2 rocks points also to some hybridization with coeval granite melts at emplacement levels. Nevertheless, the degree of crustal contribution to the composition of these non-primary mafic magmas during transport and emplacement (Gallastegui, 2005) or within the mantle source (López-Moro and López-Plaza, 2004; Orejana et al., 2020) remains an open question. Small vaugnerite bodies in the southern CIZ (Errandonea et al., 2019), coeval with voluminous peraluminous granite intrusions (305 Ma; Errandonea, 2019), suggest derivation from mantle sources with a more radiogenic Nd composition, thus defining a heterogeneous isotope Sr–Nd compositional field for monzonitic rocks, similar in extent to that defined by the rest of CALC-2 gabbros (Fig. 7A).

The issue of the degree of mafic magma contamination by interaction with felsic melts during emplacement also applies to most of the Variscan gabbros. Nevertheless, the common occurrence of olivine and clinopyroxene in the most primitive gabbros of the non-monzonitic or apinitic suites has been interpreted as incompatible with significant

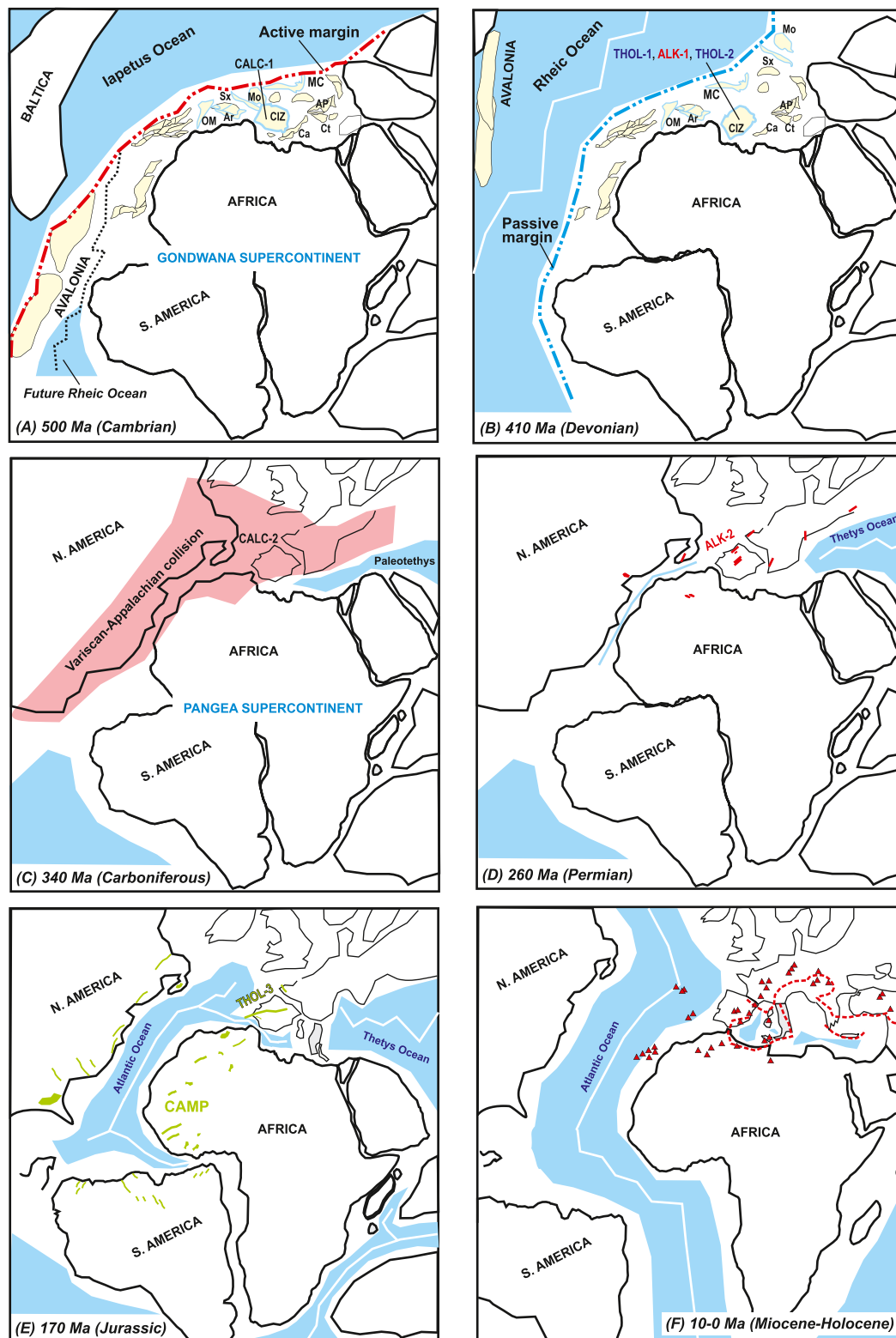


Fig. 8. Paleogeographical reconstructions of the Iberian plate during the Phanerozoic. (A) Cambrian reconstruction of the subduction peri-Gondwana margin (ca. 500 Ma) inspired in Stampfli et al. (2013). OM = Ossa Morena; Ar = Armorica; Sx = Saxothuringia; Mo = Moesia; MC = Massif Central; Ca = Cantabria; AP = Aquitaine-Pyrenees-Corsica; Ct = Catalonia. (B) Devonian development of passive margin conditions in peri-Gondwanan terranes (after Stampfli et al., 2013). (C) Variscan collision that started from 393 to 360 Ma depending on the microterran location (e.g., Stampfli et al., 2013). (D) Alkaline magmatism during Permian to Triassic showing outcrops from Orejana et al. (2020), Batki et al. (2014), Casetta et al. (2019) and Najih et al. (2019 and references therein) within a paleogeodynamic reconstruction (inspired in Van Hinsbergen et al., 2020). (E) Distribution of tholeiitic magmatism of Late Triassic to Early Jurassic in the Central Atlantic area. CAMP = Central Atlantic Magmatic Province (data from Cebriá et al., 2003; Najih et al., 2019). (F) Anorogenic (intraplate) volcanism in the circum-Mediterranean area in the last 10 Ma, modified after Lustrino and Wilson (2007) and Carminati et al. (2012).

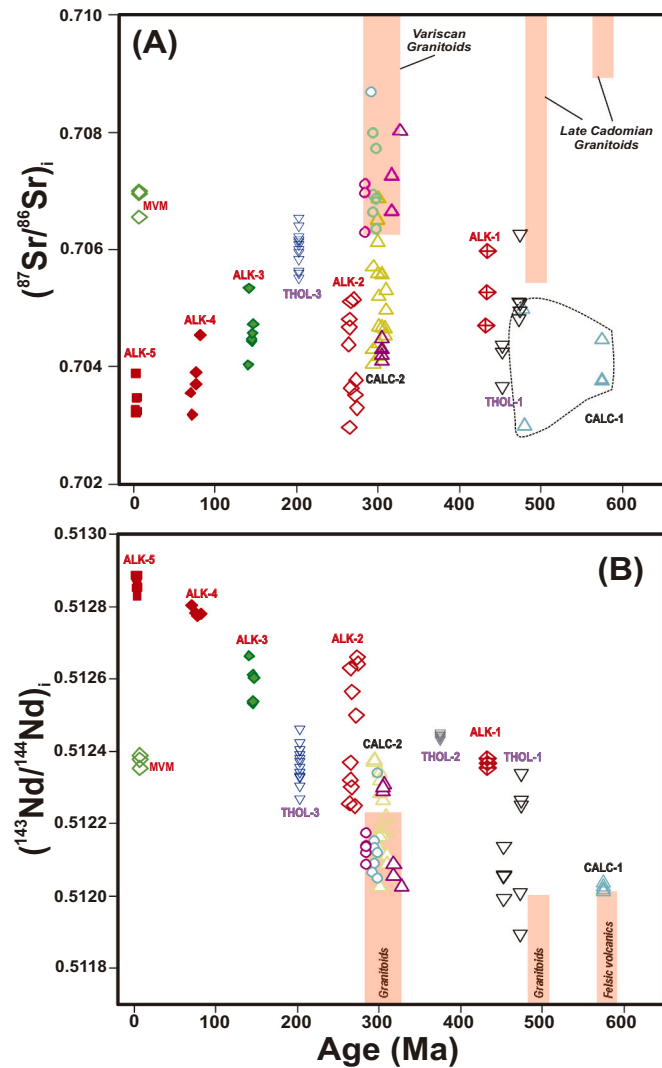


Fig. 9. Initial $^{87}\text{Sr}/^{86}\text{Sr}$ (A) and $^{143}\text{Nd}/^{144}\text{Nd}$ (B) ratios vs. time (in Ma) of mafic rocks from the CIZ. Isotopic ratios were calculated at the age of each magmatic event. Compositional fields of the Iberian felsic igneous rocks (*Late Cadomian data*: Rodríguez-Alonso et al., 2004; Antunes et al., 2009; Villaseca et al., 2016; *Variscan granitoids*: Bea et al., 1999; Dias et al., 2002; Villaseca et al., 2009; Merino Martínez et al., 2014) are plotted for comparison purposes. Note that some CALC-1 and THOL-2 rocks are not shown due to the lack of suitable published isotope data.

contamination with crustal material (e.g., Dias et al., 2002). Moreover, the lack of correlation of Sr–Nd isotopic signatures with the SiO_2 or LILE contents of the most primitive gabbros goes against significant crustal contamination during their emplacement (e.g., Orejana et al., 2009). The isotopic signatures of Variscan gabbros suggest heterogeneous lithospheric mantle sources more enriched than those from the depleted mantle or the recent Atlantic MORB (Fig. 7), as previously established (Dias et al., 2002; Scarrow et al., 2009; Orejana et al., 2009; Villaseca et al., 2011). This mantle component is very similar in Sr–Nd isotopic composition to those involved in the genesis of the CALC-1 gabbros. The strong thickening of the Central Iberian crust during the Variscan collision (70–80 km, Barbero and Villaseca, 2000), and the subsequent generation of voluminous felsic magmas, facilitated the interaction of crustal-derived components as contaminants during mafic magma transport/emplacement. An alternative possibility would be the subduction or delamination of the denser granulitic material into the lithospheric mantle (e.g., Villaseca et al., 1999; Orejana et al., 2009).

Crustal contamination of the lithospheric mantle during the complex

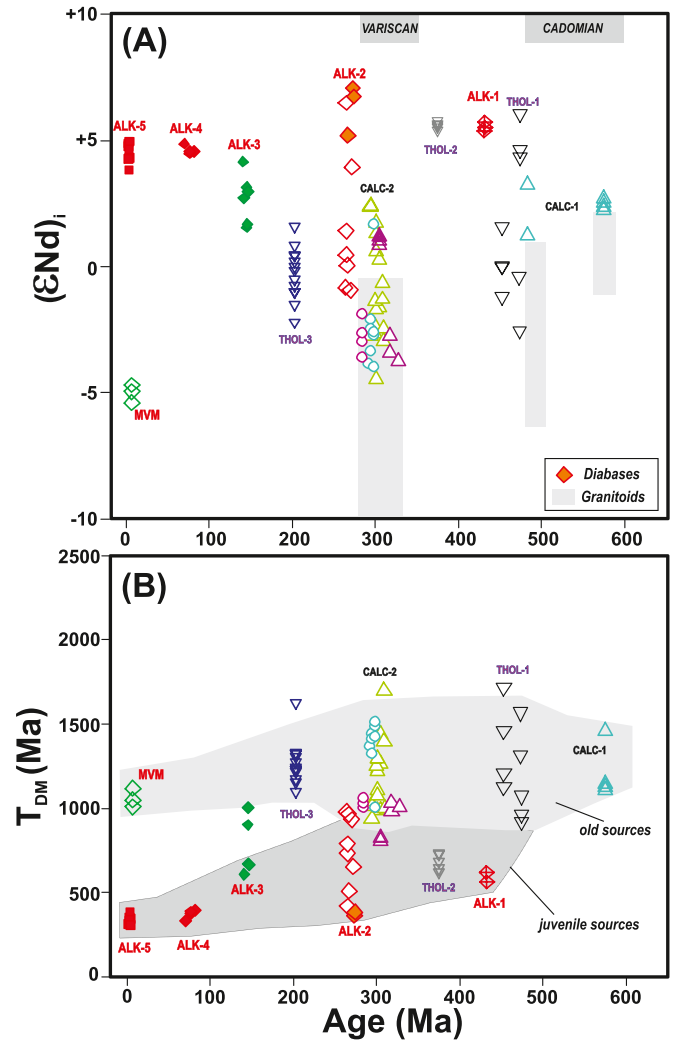


Fig. 10. Initial ϵ_{Nd} (A) and T_{DM} Nd model ages (B) vs. time (in Ma) of mafic rocks from the CIZ. Model ages are used as an estimation of the time of magma segregation from its mantle source, but in this work, as most mantle-derived magmas are from different and more enriched mantle sources, T_{DM} Nd model ages are meaningless and only used with the aim of comparison. The two orogenic cycles (Cadomian and Variscan) and the compositional range of the associated felsic magmatism (*Cadomian data*: Solá et al., 2008; Antunes et al., 2009; Villaseca et al., 2016; *Variscan data*: e.g., Bea et al., 1999; Dias et al., 2002; Villaseca et al., 2009; Merino Martínez et al., 2014) are roughly schematized. Na-rich diabases from the ALK-2 event are highlighted.

Variscan collision is apparent in the later tholeiitic (THOL-3) and alkaline (ALK-5 leucitites) series (e.g., Callegaro et al., 2014; Lustrino et al., 2019, respectively). The deep mantle was likely metasomatized by subducted continental material after the Variscan collision, as no such initial Sr radiogenic and Nd unradiogenic values were previously recorded in pre-Variscan mafic magmatic events (Fig. 9). This is an important change in the type of crust–mantle interaction beneath the CIZ as the Neoproterozoic to Early Ordovician enriched mantle sources were probably inherited from a pre-existing ancient lithospheric mantle or were metasomatized by fluids derived from the subducted Iapetus–Rheic oceanic crust.

Additionally, the 42-Ma period of monzonitic Variscan magmatism and associated granitoids implies the existence of a long-lived thermal anomaly within central Iberia to sustain a high heat flux with crustal anatexis up to the Early Permian (Gb3 monzonitic dykes of Orejana et al., 2020). The deepening in mantle melting from this K-rich late Variscan event to the posterior alkaline event (ALK-2) occurs in the

same area and in a relatively short-time of <12 Ma (Orejana et al., 2020). This suggests an important lithospheric thinning or delamination and the triggering of a complex mantle flow with asthenospheric upwelling at post-Variscan times in central Iberia (Orejana et al., 2008; Gutiérrez-Alonso et al., 2011), although the geodynamic scenario is still not totally constrained, as occurs in nearby terranes (e.g., Laurent et al., 2017).

The intrusion of alkaline magmas in central Spain during the Permian illustrates the involvement of new enriched mantle sources different to those involved in the Variscan orogenesis. This ALK-2 cycle implies the intrusion of K-rich ultrabasic-basic lamprophyres and sodic diabases, some of the latter displaying $K_2O/Na_2O < 1$ (Supplementary Table S1). The diabases have isotopic signatures close to the PREMA mantle reservoir, whereas the lamprophyres show more enriched signatures (Fig. 7A, C). The Nb/Th and Ce/Nb ratios of these ALK-2 rocks have been used to identify the presence of amphibole or phlogopite in the mantle source (e.g., Orejana et al., 2020). These geochemical ratios indicate that K-rich lamprophyres are in agreement with derivation from a phlogopite-bearing lithospheric mantle, whereas the associated diabases might be derived from sources poorer in hydrous phases (phlogopite, amphibole), similarly to other later Na-rich alkaline rocks (most of the ALK-3, -4 and -5 series) (Supplementary Fig. S3). The Sr–Nd isotopic ratios of the ALK-2 suite point to melting of lithospheric and asthenospheric mantle sources previously metasomatised by deep-seated K-volatile-rich melts (Orejana et al., 2008). The Th/Yb or Zr/Nb ratios of these ALK-2 rocks (Fig. 6A, D) preclude a main role of recent crustal components (either from continental or oceanic derivation), being more likely the melting of OIB-like sources with enrichment related to old reservoirs (Orejana et al., 2008, 2020). It is worth noting the overlapping of the ALK-2 rocks incompatible trace element ratios with compositional fields of later alkaline suites of EAR mantle derivation (e.g., Fig. 6A, B), in agreement with the model of the rising of deep convecting asthenospheric mantle in the context of continental rifting (Orejana et al., 2020). Moreover, they show similar Zr/Nb and Nb/Th ratios to those of other OIB rocks from the Atlantic realm (later ALK-4 suite, Fig. 6C), suggesting the early incoming during Permian times of mantle instabilities similar to small plumes or diapirs (Condie, 2005). Accordingly, the ALK-2 suite could be considered the first hints of the later dominant Atlantic EAR component (e.g., Fig. 7B, C).

All these data suggest that this 274–265 Ma ALK-2 magmatism might be considered within the context of the continental breakdown of the Pangea supercontinent and the opening of the oceans that surround Iberia (Tethys and Atlantic) (Fig. 8D). Numerous alkaline intrusions and tectonothermal events have been recorded during the Permian and the Triassic in southern Europe, related to the extensional stages of the proto-Alpine Tethys rift (e.g., Thöni and Miller, 2009; Batki et al., 2014; Casetta et al., 2019). Owing to this destruction of the Variscan roots and regional uplift, the widespread thinning of the Variscan lithosphere might have triggered a reorganization of the asthenospheric flow patterns (Ziegler et al., 2004). Moreover, the presence of late Permian small-volume alkaline magmatism on both sides of the future Atlantic Ocean remarks the complex rifting of the Variscan orogen in different branches (Ross, 2010; Najih et al., 2019). The intrusion of Permian alkaline lamprophyres about 264–252 Ma in the Moroccan Anti-Atlas of the West African Craton (Najih et al., 2019), a continental terrane very close to the Iberian plate after the Variscan collision, also suggests the onset of rifting in other circum-Mediterranean regions, which would give rise to the future Atlantic Ocean frontage (Fig. 8D). These alkaline events predate by about 35 to 70 Ma the Triassic–Jurassic Central Atlantic rifting and the subsequent associated tholeiitic magmatism.

The reconstruction of the Central Atlantic opening is a challenging task, but recent works, mainly based on timing of oceanic magnetic anomalies and rift-related magmatism, place the starting stages at ca. 195 Ma (e.g., Van Hinsbergen et al., 2020 and references therein). Nevertheless, the beginning of the Atlantic rifting in SW Iberia is believed to occur during the Late Triassic (228 to 204 Ma), 20 to 30 Ma

before magmatism, as deduced from rift-related sedimentation (Martins et al., 2008). The great tholeiitic Messejana-Plasencia dyke and the volcanic successions of the Algarve Basin (THOL-3 suite) have been linked to the Central Atlantic Magmatic Province (e.g., Cebriá et al., 2003; Martins et al., 2008, Fig. 8E). These tholeiitic mafic rocks have been interpreted as the result of partial melting of enriched lithospheric mantle sources (Cebriá et al., 2003; Callegaro et al., 2014). The isotope variation observed through the Messejana-Plasencia dyke length indicates that it was not emplaced during a single episode of intrusion, but by a number of injections over a relatively short period of time (<1 Ma, Palencia Ortas et al., 2006). The oldest part of the dyke corresponds to the northern segment in central Spain, the region where continental crust reached its maximum thickening during the Variscan, and where subsequent granulite delamination into the mantle has been invoked (Villaseca et al., 1999). This segment is also the most enriched in radiogenic Sr and unradiogenic Nd isotope ratios (Fig. 7A), features explained by continental crustal contamination (i.e., lower crustal granulites) (Cebriá et al., 2003). The tholeiitic dyke is slightly younger towards SW Portugal (Schermerhorn et al., 1978), where it intruded into a thinner continental crust, displaying Sr–Nd isotopic ratios closer to a BSE mantle composition (Fig. 7A).

From Late Mesozoic to Cenozoic, the Iberian plate (not only the CIZ) registered several cycles of sporadic intraplate magmatism of alkaline affinity (e.g., Mata et al., 2015; Villaseca et al., 2019). A first cycle of mafic mildly alkaline to subalkaline rocks during Late Jurassic–Early Cretaceous (148–140 Ma; ALK-3) is followed by Late Cretaceous (94–69 Ma; ALK-4) sporadic alkaline magmatic events, also in the western Iberian margin. A third episode includes the recent Cenozoic volcanic fields (< 8 Ma), such as the studied Calatrava field in central Iberia (Fig. 8). These Na-rich alkaline magmatic cycles show a progressive chemical evolution from transitional subalkaline rocks to younger silica-undersaturated magmas with EAR-like isotopic values. Thus, the youngest and more alkaline gabbros of the southern Lusitanian block (e.g., BL24 sample in Supplementary Table S2) show the highest radiogenic Nd and lowest radiogenic Sr isotope ratios among the ALK-3 rocks, close to the compositional fields of ALK-4 and ALK-5 rocks (e.g., Fig. 7A). These features agree with the progressive increase in LREE/HRRE ratios of the Mesozoic to Cenozoic alkaline series (increasing depth of melting) and the incoming of asthenospheric sources of EAR composition from Late Cretaceous to the present, which has become the dominant mantle component in the intraplate magmatism of the western circum-Mediterranean areas (Lustrino and Wilson, 2007). The study of metasomatic events in lherzolite xenoliths of the subcontinental lithospheric mantle beneath central Iberia also supports the increasingly abundance of silica-undersaturated EAR-like magmas in the successive alkaline magmatic events (including carbonatites) during the last ca. 118 Ma (Villaseca et al., 2019). Thus, although in some diagrams most alkaline suites plot in fields of asthenospheric affinity (e.g., Figs. 4A and 5A), only those silica-undersaturated rocks with PREMA or EAR isotope features (i.e., diabases from ALK-2, ALK-4 and Na-rich volcanics of ALK-5 suites) have been documented as derived from the asthenosphere. In fact, Permian diabases (Orejana et al., 2008) and post-Cretaceous Na-rich alkaline rocks were related to partial melting of sublithospheric sources subsequently contaminated by percolation through the metasomatized Iberian subcontinental lithospheric mantle (e.g., Grange et al., 2010; Cebriá and López Ruiz, 1995).

The presence of a K-rich volcano in the Calatrava volcanic field of central Spain (and also of K-rich lamproites in southeastern Spain, similar in age and chemical composition) points to the existence of strongly enriched lithospheric components within deep mantle levels, in accordance with subduction and delamination models proposed for the post-collisional Variscan stages. Generation of low melt fractions by partial melting of deep mantle levels (even within the asthenosphere) may have been triggered by reorganization of mantle flow patterns during the Early Cenozoic collision of Africa with Europe (Alpine orogeny). The data available from the singular leucititic volcano of the

Calatrava field suggest the involvement of a mixture of mantle components: a convecting EAR-like mantle with an Iberian lithospheric source displaying geochemical features compatible with recycling of variable crustal components (see for instance, Fig. 7A, C), as also suggested by Lustrino et al. (2019) for these same rocks.

5.2. Comparison with Neoproterozoic to Cenozoic mafic magmatism of central Europe terranes

Recent works on the Sm–Nd isotopic evolution of the mantle sources in continental Europe over extended periods of time (pre-Variscan, Variscan to Cenozoic cycles) (e.g., Dostal et al., 2019b) enable the comparison of their geochemical features with those of the Phanerozoic mafic magmatism described above for central Iberia (Fig. 11). These data, combined with other geochemical and isotopic characteristics of central Europe mafic rocks (Dostal et al., 2019a; Krmíčková et al., 2020), can enhance this comparison.

The main differences between the mantle sources of the mafic magmatism of central European terranes and those from the central Iberia mostly occur in pre-Variscan times, when higher variable magmatic activity occurred during a longer age range (up to 600 Ma ago). The Nd model ages and the more radiogenic Nd values (most of $\epsilon_{\text{Nd}}(t) > +3$; Fig. 11) indicate that mafic magmas from central Europe come from more juvenile and depleted mantle sources (mostly of oceanic N-MORB affinity) with no indications of significant crustal contamination (Dostal et al., 2019a). On the contrary, the first CIZ calc-alkaline and tholeiitic magmatic events (CALC-1 and THOL-1) display more radiogenic Nd values rarely exceeding $\epsilon_{\text{Nd}}(t)$ of +6, while extending towards slightly negative values (up to –2.6 in THOL-1 from El Caloco massif, Orejana et al., 2017), values unreported in central European terranes (Fig. 11). These chemical differences suggest that central Europe terranes would be located farther from continental areas than central Iberia, possibly as a peri-Gondwanan terrane in the most external continental edge or adjacent to an island arc. This possibility agrees with most of the paleogeographic reconstructions from Late Neoproterozoic to Cambrian times, which place the Bohemian Massif

and other European terranes (e.g., Armorica) along the northernmost Gondwanan margin (e.g., Von Raumer et al., 2013; Stampfli et al., 2013) (Fig. 8A and B). In addition, the Cadomian orogeny seems to have perturbed more strongly the subcontinental mantle in southern Europe than in northernmost areas. Large volumes of crustal-recycled felsic magmas were generated in Iberia during a wider (and younger) time span (500–480 Ma, Villaseca et al., 2016), whereas in central Europe the Cadomian magmatism was related to a more classic oceanic subduction setting that ended at about 540 Ma (e.g., Dostal et al., 2019b). Moreover, the Late Cambrian to Early Ordovician (500–478 Ma) mafic magmatism from central Europe involved mantle upwelling in the context of the opening of the Rheic Ocean (e.g., Dostal et al., 2019b). The scarcity of Early Ordovician metabasites in the Central Iberian Zone does not support a widespread rifting scenario in this microplate at that time, as this terrane was located further to the main extensional area (Fig. 8A and B).

The Nd isotope composition of mafic igneous series of central Europe and Iberia displays a stronger resemblance during and after Variscan times. The influence of this collision in the associated mafic magmatism is manifested by an abrupt change in the radiogenic Nd values associated with this orogenic event in central Europe, marked by negative $\epsilon_{\text{Nd}}(t)$ values (up to –7) and significantly high Nd model ages (up to 1800 Ma) in Variscan gabbros (Dostal et al., 2019b). These results reflect the overlapping of Nd composition (and model ages) of Variscan basic rocks from both sectors (Fig. 11). The assemblage of European basement terranes during Late Paleozoic consolidates a European continent, where subsequent proto-oceanic riftings (Tethys and Atlantic) would induce similar mantle-derived magmatic events in these welded terranes. As an example, intraplate Na-alkaline rocks from the Mesozoic to present times have very similar Nd–Pb isotopic signatures in both sections of continental Europe (compare Fig. 7B–C with data from Krmíčková et al., 2020). Nevertheless, the incoming of post-Variscan alkaline events derived from sublithospheric sources (PREMA to EAR components), since the Permian in central Iberia and NW Morocco, occurs some 70 Ma earlier than in other western European terranes.

There are other two notable differences in the characteristics of post-Variscan mafic magmas between Iberia and central Europe. The first is associated with the incoming of tholeiitic magmatism during Late Triassic–Jurassic in Iberia, which is not recorded in central Europe due to its remoteness to the incipient Atlantic costline. Only a minor dyke swarm of coeval tholeiitic diabases appears in the westernmost Armorican Massif, in France (Caroff et al., 1995) (Fig. 8E). The second refers to the scarcity of post-Variscan mafic magmas of lithospheric derivation in central Europe, which contrasts with the relative abundance of K-rich leucites and lamproites in the Iberian plate and other southern European circum-Mediterranean terranes. Although some Cenozoic K-rich volcanic rocks appear in central Europe (e.g., Lustrino et al., 2019), they have more unradiogenic Sr and radiogenic Nd isotope ratios (plotting in the BSE compositional field) far from the compositional field of CIZ leucites (MVM samples in Fig. 7A), suggesting the involvement of deeper mantle sources.

These differences, along with the higher lithospheric contribution shown by the northern segment of the Late Triassic tholeiitic dyke (THOL-3 rocks), suggest a higher degree of crustal contamination of the Iberian subcontinental mantle after the Variscan collision than in central European terranes (Fig. 11). It seems that the described crust–mantle decoupling of central European terranes during the Variscan (Dostal et al., 2019a, 2019b) is not so evident in Iberia, where an enriched subcontinental lithospheric mantle (Fig. 11) is apparently maintained after this collision. Moreover, the Alpine collision has not been significant in central Europe, whereas it is concentrated in the circum-Mediterranean area, where multiple crustal microplates have been subducted during this long-lasting orogeny (mainly during the last 55 Ma), generating a complex lithospheric/asthenospheric mantle flow and associated orogenic K-rich volcanic areas like the one in SE Spain (e.g., Carminati et al., 2012). The geochemical features of the CIZ leucites

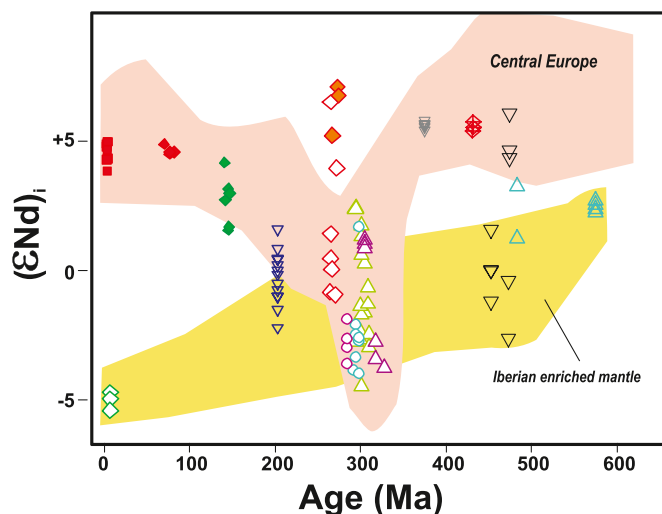


Fig. 11. Initial ϵ_{Nd} vs. time of the mafic Neoproterozoic to Cenozoic magmatism of central Europe (compositional field from data of Dostal et al., 2019b) compared to those occurring in the Iberian plate (from Fig. 10 above). The field of unradiogenic Nd isotope ratios of studied mafic magmatism defines an enriched lithospheric subcontinental mantle in central Iberia that in central Europe does not appear. Only intraplate Na-rich alkaline magmatism after Variscan collision have geochemical features similar in both European basement terranes. Compositional field of the mafic magmatism from the central European Variscan Belt present a large overlap with our data set. See text for further explanation. Same symbols as in Fig. 10.

(relative depletion of Ba and Sr, and high Th, U contents combined with radiogenic Sr, unradiogenic Nd and high $^{207}\text{Pb}/^{204}\text{Pb}$ ratios) differ from anorogenic lamproites (Casalini et al., 2021), being instead indicative of a subduction-related signature, typical of the western Mediterranean (Tethyan) lamproites.

Further studies are necessary to constrain the nature of enrichment in the subcontinental lithospheric mantle of central Iberia from Neoproterozoic times. Probably the persistence of enriched mantle sections during such a long period is consequence of feedback processes related to crustal recycling and granulite delamination, along with tectonic erosion and crustal subduction during the Cadomian and Variscan orogenies (e.g., Orejana et al., 2009; Gutiérrez-Alonso et al., 2011). Alternatively, part of this enrichment could be an old feature preserved in the Iberian subcontinental mantle, later recycled by mantle flow instabilities during the successive extensional events between orogenic cycles. The isotopic features of the central Iberian pre-Variscan sub-alkaline mafic magmas and the presence of inherited Proterozoic zircons in metabasites of THOL-1 suites (Orejana et al., 2017) might support this second alternative and the existence of an old pre-Phanerozoic Iberian enriched mantle (Fig. 11), not found in central Europe.

5.3. Subcontinental lithospheric mantle beneath western Europe from xenolith suites studies

The successive events of mafic magmatism in central Iberia have left a limited record in mantle xenoliths from the only region where these appear: the Calatrava Volcanic Field. The $\text{Re}-\text{Os}$ isotope systematics performed on mantle sulfides of these lherzolite xenoliths yield Re-model ages from 1.8 to 0.3 Ga, which have been related to supercontinental assembly events (e.g., the Cadomian and Variscan orogenic cycles; González-Jiménez et al., 2013). Similar results have been obtained in other European xenolith suites (e.g., Alard et al., 2002). Recent studies on the Calatrava mantle xenoliths have described the presence of metasomatic imprints of tholeiitic (García Serrano et al., 2021), subduction-related (Villaseca et al., 2022) or alkaline melts (Villaseca et al., 2010; González-Jiménez et al., 2014) that have percolated the Calatrava subcontinental mantle in different stages. Nevertheless, the available geochronological data (Villaseca et al., 2019) only record alkaline metasomatic events, which correspond to three successive metasomatic stages of Cretaceous (118 Ma), Oligocene (29 Ma) and Miocene (16–4 Ma) ages. The two most recent alkaline events did not reach the surface of central Iberia showing that a significant part of mantle-derived magmatism leaves no trace in overlying crustal levels.

A similar outline is inferred from studies on mantle xenoliths from Cenozoic volcanoes of western and central Europe (e.g., Puziewicz et al., 2020). Three major types of subcontinental lithospheric mantle have been established: a Variscan orogenic depleted mantle with evidence of metasomatism by subduction-related agents, a Cenozoic rifted mantle strongly metasomatized by prolonged alkaline events, and a refertilized mantle by post-Variscan asthenosphere upwelling of uncertain age. As in central Iberia, the study of xenolith suites from Variscan European terranes suffers from the lack of in situ geochronological approaches and the strong modifications induced by the long-lasting and multi-phase Cenozoic alkaline volcanism of the European volcanic fields (e.g., Uenver-Thiele et al., 2017). This makes difficult to attain a comprehensive and satisfactory correlation between metasomatic processes identified in mantle xenoliths and the outcropping mafic magmatism, and to achieve a detailed knowledge of the evolution of the subcontinental lithospheric mantle beneath the European terranes.

6. Conclusions

In the central domain of the Iberian Peninsula, ten mafic magmatic episodes from the Neoproterozoic to the present time have been characterized based on a compilation of immobile trace element and isotope (Sr–Nd–Pb) data. Within this 575 Ma age range two orogenic events have

been recognized (Cadomian subduction and Variscan continental collision cycles) displaying scarce mafic calc-alkaline magmatism. These orogenic events gave way to eight intraplate alkaline or tholeiitic mantle inputs. The geochemical evolution of these mafic rocks indicates that asthenospheric and lithospheric mantle sources were involved during the successive melting events and that significant subduction of crustal components occurred during the assemblage of the last two supercontinents (Gondwana and Pangea) and their subsequent breakdown.

The mafic intrusions associated to these two orogenic cycles represent calc-alkaline series subordinate to a much larger felsic magmatism, which highlights the major relevance of intracrustal recycling following convergence and crustal thickening. The minor crustal signatures shown by most of the post-Variscan mantle-derived magmas (only THOL-3 and the leucitites associated to ALK-5 rocks show enriched isotopic ratios), are indicative of the main role played by asthenospheric mantle sources uprising from Permian to present times. On the other hand, the involvement of enriched lithospheric mantle sources during the Cadomian and Variscan orogenies, and occasionally during post-Variscan stages, implies the existence of an older (Proterozoic?) subcontinental mantle beneath central Iberia.

The northernmost central European basement terranes involve the melting of more juvenile and depleted mantle sources before the Variscan cycle, suggesting a location closer to the oceanic margin of Gondwana when compared to the position of the CIZ terranes. Thus, the change towards higher radiogenic Nd isotopic signatures and model ages associated with the Variscan orogeny is more abrupt in northern Europe than in central Iberia. This collisional event implies the intrusion of calc-alkaline mafic magmas with broadly similar composition in all considered European terranes. A substantial crust-mantle interaction is observed during this collision.

Significant similarities exist between the post-Variscan mafic magmatism of southwestern and central European terranes, although minor episodes of intraplate magmatism involving moderately to strongly enriched lithospheric mantle sources (tholeiitic and K-rich magmas) are restricted to the southernmost Mediterranean Europe where Africa and Eurasia convergence is prevalent.

The current poor record of successive metasomatic events from direct sampling of the western Europe subcontinental lithospheric mantle (peridotite xenoliths) does not reflect the complexity of outcropping magmatic events in these areas. Moreover, some alkaline metasomatic events of Cenozoic age, dated in mantle xenoliths from central Iberia, lack shallower magmatic equivalents. This limits the correlation between outcropping mafic magmatism and the scarce record of old metasomatic events within the underneath lithospheric mantle.

Declaration of Competing Interest

The authors declare that the submitted work was carried out without the presence of any personal or professional relationships that could potentially be construed as a conflict of interest or competing financial interests.

Acknowledgments

We want to acknowledge José Manuel Fuenlabrada and Virginia Sánchez from the CAI-UCM of Isotope Geochemistry and Geochronology for their help in Sr–Nd data acquisition. We are grateful to the suggestions made by M^a José Huertas on a previous draft. We also greatly appreciate the comments and suggestions made by Joao Mata and Sonja Aulbach during the revision of a first version of the manuscript that greatly improved the quality of this study. This work is included in the objectives of, and supported by, the CGL2016-78796 and the PID2020-115980GB-I00 projects of the Ministerio de Ciencia e Innovación de España, and the 910492 and 971008 UCM groups.

Appendix A. Supplementary data

Supplementary data to this article can be found online at <https://doi.org/10.1016/j.earscirev.2022.103997>.

References

- Alard, O., Griffin, W.L., Pearson, N.J., Lorand, J.P., O'Reilly, S.Y., 2002. New insights into the Re-Os systematics of sub-continental lithospheric mantle from in situ analysis of sulphides. *Erath Planet. Lett.* 203, 651–663.
- Ancochea, E., Huertas, M.J., 2021. Radiometric ages and time-space distribution of volcanism in the Campo de Calatrava Volcanic Field (Iberian Peninsula). *J. Iber. Geol.* 47, 209–223.
- Antunes, I.M.H.R., Neiva, A.M.R., Silva, M.M.V.G., Corfu, F., 2009. The genesis of I- and S-type granitoid rocks of the early Ordovician Oledo pluton, Central Iberian Zone (Central Portugal). *Lithos* 111, 168–185.
- Axen, G.J., van Wijk, J.W., Currie, C.A., 2018. Basal continental mantle lithosphere displaced by flat-slab subduction. *Nat. Geosci.* 11, 961–964.
- Ballèvre, M., Martínez Catalán, J.R., López-Carmona, A., Pitra, P., Abati, J., Díez Fernández, R., Ducassou, C., Arenas, R., Bosse, V., Castiñeiras, P., Fernández-Suárez, J., Gómez Barreiro, J., Paquette, J.L., Peucat, J.J., Poujol, M., Ruffet, G., Sánchez Martínez, S., 2014. Correlation of the nappe stack in the Ibero-Armorican arc across the Bay of Biscay: a joint French-Spanish project. In: Schulmann, K., Martínez Catalán, J.R., Lardeaux, J.M., Janousek, V., Oggiano, G. (Eds.), *The Variscan Orogeny: Extent, Timescale and the Formation of the European Crust*, 405. Geol. Soc. London, Spec. Publ. pp. 77–113.
- Bandrés, A., Eguíluz, L., Pin, C., Paquette, J.L., Ordóñez, B., Le Fèvre, B., Ortega, L.A., Gil Ibaguchi, J.I., 2004. The northern Ossa-Morena Cadomian batholith (Iberian Massif): magmatic arc origin and early evolution. *Int. J. Earth Sci.* 93, 860–885.
- Barbero, L., Villaseca, C., 2000. Eclogite facies relics in metabasites from the Sierra de Guadarrama (Spanish Central System): P-T estimations and implications for the Hercynian evolution. *Min. Mag.* 64, 815–836.
- Batki, A., Pál-Molnár, E., Dobosi, G., Skelton, A., 2014. Petrogenetic significance of ocellar camptonite dykes in the Ditrău Alkaline Massif, Romania. *Lithos* 200, 181–196.
- Baudouin, C., Parat, F., 2020. Phlogopite-olivine nephelinites erupted during Early Stage Rifting, North Tanzania Divergence. *Front. Earth Sci.* 8, 277.
- Bea, F., Montero, P., Molina, J.F., 1999. Mafic precursors, peraluminous granitoids, and late lamprophyres in the Avila batholith: a model for the generation of Variscan batholiths in Iberia. *J. Geol.* 107, 399–419.
- Bea, F., Gallastegui, G., Montero, P., Molina, J.F., Scarrow, J., Cuesta, A., González-Menéndez, L., 2021. Contrasting high-Mg, high-K rocks in Central Iberia: the appinite-vaugnerite conundrum and their (non-existent) relation with arc magmatism. *J. Iber. Geol.* 47, 235–261.
- Bernard-Griffiths, J.B., Gruau, G., Cornen, G., Azambre, B., Macé, J., 1997. Continental lithospheric contribution to alkaline magmatism: Isotopic (Nd, Sr, Pb) and geochemical (REE) evidence from Sierra de Monchique and Mount Ormonde complexes. *J. Petrol.* 38, 115–132.
- Boynton, W.V., 1985. Geochemistry of the rare earth elements: Meteorite studies. In: Henderson, P. (Ed.), *Rare Earth Element Geochemistry*. Elsevier, New York, NY, pp. 63–114.
- Brandl, P.A., Genske, F.S., Beier, C., Haase, K.M., Sprung, P., Krumm, S.H., 2015. Magmatic evidence from carbonate metasomatism in the lithospheric mantle underneath the Ohre (Eger) Rift. *J. Petrol.* 56, 1743–1774.
- Callegaro, S., Rapaille, C., Marzoli, A., Bertrand, H., Chiarada, M., Reisberg, L., Bellieni, G., Martins, L., Madeira, J., Mata, J., Youbi, N., De Min, A., Azevedo, M.R., Bensalah, M.K., 2014. Enriched mantle source for the Central Atlantic magmatic province: new supporting evidence from southwestern Europe. *Lithos* 188, 15–32.
- Cambeses, A., Scarrow, J.H., Montero, P., Lázaro, C., Bea, F., 2017. Palaeogeography and crustal evolution of the Ossa-Morena Zone, Southwest Iberia, and the North Gondwana margin during the Cambro-Ordovician: a review of isotopic evidence. *Int. Geol. Rev.* 59, 94–130.
- Carminati, E., Lustrino, M., Doglioni, C., 2012. Geodynamic evolution of the central and western Mediterranean: tectonics vs. igneous petrology constraints. *Tectonophysics* 579, 173–192.
- Caroff, M., Bellon, H., Chauris, I., Chevriér, S., Gardinier, A., Cotton, J., Moan, Y.L., Neidhart, Y., 1995. Magmatisme fissural triasico-liasique dans l'ouest du Massif Armoricain (France): pétrologie, géochimie, âge, et modalités de la mise en place. *Can. J. Earth Sci.* 32, 1921–1936.
- Casalini, M., Avanzinelli, R., Tommasini, S., Natali, C., Bianchini, G., Prelevic, D., Matteir, M., Conticelli, S., 2021. Petrogenesis of Mediterranean lamproites and associated rocks: the role of overprinted metasomatic events in the postcollisional lithospheric upper mantle. *Geol. Soc. London Spec. Publ.* 513. <https://doi.org/10.1144/SP513-2021-36>.
- Casetta, F., Ickert, R.B., Mark, D.F., Bonadiman, C., Giacomoni, P.P., Ntafos, T., Coltorti, M., 2019. The alkaline lamprophyres of the Dolomitic area (Southern Alps, Italy): markers of the late Triassic change from orogenic-like to anorogenic magmatism. *J. Petrol.* 60, 1263–1298.
- Cebriá, J.M., López Ruiz, J., 1995. Alkali basalts and leucitites in an extensional intracontinental plate setting: the late Cenozoic Calatrava volcanic province (Central Spain). *Lithos* 35, 27–46.
- Cebriá, J.M., Wilson, M., 1995. Cenozoic mafic magmatism in Western/Central Europe: a common European asthenospheric reservoir. *Terra Nova Abstract Suppl.* 7, 162.
- Cebriá, J.M., López-Ruiz, J., Doblas, M., Martins, L.T., Munha, J., 2003. Geochemistry of the early Jurassic Messejana-Plasencia dyke (Portugal-Spain): implications on the origin of the Central Atlantic Magmatic Province. *J. Petrol.* 44, 547–568.
- Civiero, C., Custódio, S., Neres, M., Schlaphorst, D., Mata, J., Silveira, G., 2021. The role of the seismically slow Central-East Atlantic Anomaly in the genesis of the Canary and Madeira Volcanic Provinces. *Geophys. Res. Lett.* 48, e2021GL092874.
- Condie, K.C., 2005. High field strength element ratios in Archean basalts: a window to evolving sources of mantle plumes? *Lithos* 79, 491–504.
- Cotrim, B., Bento dos Santos, T., Mata, J., Benoit, M., Jesus, A.P., 2021. Lower Paleozoic rifting event in Central Iberian Zone (central-North Portugal): evidence from elemental and isotopic geochemistry of metabasic rocks. *Geochemistry* 81, 125768.
- Dewey, J.F., 1988. Extensional collapse of orogens. *Tectonics* 7, 1123–1139.
- Dias da Silva, I., Valverde-Vaquero, P., González-Clavijo, E., Díez-Montes, A., Martínez-Catalán, J.R., 2014. Structural and stratigraphical significance of U-Pb ages from the Mora and Saldanha volcanic complexes (NE Portugal, Iberian Variscides). In: Schulmann, K., Martínez-Catalán, J.R., Lardeaux, J.M., Janousek, V., Oggiano, G. (Eds.), *The Variscan Orogeny: Extent, Timescale and Formation of the European Crust*, 405. Geol. Society, London, Special Publication, pp. 115–135.
- Dias, G., Simoes, P.P., Ferreira, N., Leterrier, J., 2002. Mantle and crustal sources in the genesis of late-Hercynian granitoids (NW Portugal): Geochemical and Sr-Nd isotopic constraints. *Gondwana Res.* 2, 287–305.
- Dostal, J., Murphy, J.B., Shellnutt, J.G., Ulrych, J., Fediuk, F., 2019a. Neoproterozoic to Cenozoic magmatism in the central part of the Bohemian Massif (Czech Republic): isotopic tracking of the evolution of the mantle through the Variscan orogeny. *Lithos* 326–327, 358–369.
- Dostal, J., Murphy, J.B., Shellnutt, J.G., 2019b. Secular isotopic variation in lithospheric mantle through the Variscan orogeny: Neoproterozoic to Cenozoic magmatism in continental Europe. *Geology* 47, 637–640.
- Dunn, A.M., Reynolds, P.H., Clarke, B., Ugidos, J.M., 1998. A comparison of the age and composition of the Shelburne dyke, Nova Scotia, and the Messejana dyke, Spain. *Can. J. Earth Sci.* 35, 1110–1115.
- Dupuy, C., Liotard, J., Dostal, J., 1992. Zr/Hf fractionation in intraplate basaltic rocks: carbonate metasomatism in the mantle source. *Geochim. Cosmochim. Acta* 56, 2417–2423.
- Errandonea, J., 2019. Petrology of cordierite-bearing monzogranites and related mesocratic rocks from the Sierra Bermeja Pluton (southern Iberian Massif). In: Ph.D. dissertation. Universidad del País Vasco, Bilbao, p. 286.
- Errandonea, J., Sarrionandia, F., Carracedo-Sánchez, M., Gil Ibaguchi, J.I., Eguíluz, L., 2018. Petrography and geochemistry of late- to post-Variscan vaugnerites series rocks and calc-alkaline lamprophyres within a cordierite-bearing monzogranite (the Sierra Bermeja Pluton, southern Iberian Massif). *Geol. Acta* 16, 237–255.
- Errandonea, J., Sarrionandia, F., Janousek, V., Carracedo-Sánchez, M., Gil Ibaguchi, J.I., 2019. Origin of cordierite-bearing monzogranites from the southern Central Iberian Zone – Inferences from the zoned Sierra Bermeja Pluton (Extremadura, Spain). *Lithos* 342–343, 440–462.
- Foley, S.F., Fisher, T.P., 2017. An essential role for continental rifts and lithosphere in the deep carbon cycle. *Nat. Geosci.* 10, 897–902.
- Foley, S.F., Link, K., Tiberindwa, J.V., Barifajio, E., 2012. Patterns and origin of igneous activity around the Tanzanian craton. *J. Afr. Earth Sci.* 62, 1–18.
- Gallastegui, G., 2005. Petrología del macizo granodiorítico de Bayo-Vigo (Provincia de Pontevedra, España). In: *Serie NOVA TERRA* 26. Coruña, Edición de Castro, p. 414.
- García Serrano, J., Villaseca, C., Pérez-Soba, C., 2021. Depleted xenoliths from the leucititic Morrón de Villamayor volcano (Calatrava volcanic field, Spain). *Lithos* 380–381, 105830.
- García-Arias, M., Díez-Montes, A., Villaseca, C., Blanco-Quintero, I.F., 2018. The Cambro-Ordovician Olla de Sapo magmatism in the Iberian Massif and its Variscan evolution: a review. *Earth Sci. Rev.* 176, 345–372.
- González-Jiménez, J.M., Villaseca, C., Griffin, W.L., Belousova, E., Konc, Z., Ancochea, E., O'Reilly, S.Y., Pearson, N.J., Garrido, C.J., Gervilla, F., 2013. The architecture of the European-Mediterranean lithosphere: a synthesis of the Re-Os evidence. *Geology* 41, 547–550.
- González-Jiménez, J.M., Villaseca, C., Griffin, W.L., O'Reilly, S.Y., Belousova, E., Ancochea, E., Pearson, N.J., 2014. Significance of ancient sulphide PGE and Re-Os signatures in the mantle beneath Calatrava, Central Spain. *Contrib. Mineral. Petrol.* 168, 1047.
- Grange, M., Schärer, U., Cornene, G., Girardeau, J., 2008. First alkaline magmatism during Iberia-Newfoundland rifting. *Terra Nova* 20, 494–503.
- Grange, M., Schärer, U., Merle, R., Girardeau, J., Cornen, G., 2010. Plume-lithosphere interaction during migration of cretaceous alkaline magmatism in SW Portugal: evidence from U-Pb ages and Pb-Sr-Hf isotopes. *J. Petrol.* 51, 1143–1170.
- Granja, J.L., Vegas, R., Sentre, M.A., Muñoz-Martín, A., Sainz-Maza, S., 2015. Gravity modelling of the lithosphere in the Calatrava Volcanic Province (Spain): Geodynamic implications. *J. Iber. Geol.* 41, 233–252.
- Gutiérrez-Alonso, G., Murphy, J.B., Fernández-Suárez, J., Hamilton, M.A., 2008. Rifting along the northern Gondwana margin and the evolution of the Rheic Ocean: a Devonian age for the El Castillo volcanic rocks (Salamanca, Central Iberian Zone). *Tectonophysics* 461, 157–165.
- Gutiérrez-Alonso, G., Murphy, J.B., Fernández-Suárez, J., Weil, A.B., Franco, M.P., Gonzalo, J.C., 2011. Lithospheric delamination in the core of Pangea: Sm-Nd insights from the Iberian mantle. *Geology* 39, 155–158.
- Gutiérrez-Marco, J.C., Robardet, M., Rábano, I., Sarmiento, G.N., San José, M.A., Herranz, P., Pieren, A.P., 2002. Ordovician. In: Gibbons, W., Moreno, T. (Eds.), *The Geology of Spain*. Geological Society, London, pp. 31–49.
- Gutiérrez-Marco, J.C., Piçarra, J.M., Meireles, C.A., Cózar, P., García-Bellido, D.C., Pereira, Z., Vaz, N., Pereira, S., Lopes, G., Oliveira, J.T., Quesada, C., Zamora, S., Esteve, J., Colmenar, J., Bernárdez, E., Coronado, I., Lorenzo, S., Sá, A.A., Dias da

- Silva, I., González-Clavijo, E., Díez-Montes, A., Gómez-Barreiro, J., 2019. Early Ordovician-Devonian passive margin stage in the Gondwanan units of the Iberian Massif. In: Quesada, C., Oliveira, J.T. (Eds.), *The Geology of Iberia: A Geodynamic Approach*, Volume 2: The Variscan Cycle. Regional Geology Reviews, Springer Nature Switzerland AG 2019, pp. 75–98.
- Higueras, P., Oyarzun, R., Lillo, J., Morata, D., 2013. Intraplate mafic magmatism, degasification, and deposition of mercury: the giant Almadén mercury deposit (Spain) revisited. *Ore Geol. Rev.* 51, 93–102.
- Hofmann, A., 1997. Mantle geochemistry: the message from oceanic volcanism. *Nature* 385, 219–229.
- Huertas, M.J., Villaseca, C., 1994. Les derniers cycles magmatiques posthercyniens du Système Central Espagnol: les essais filoniens calco-alcalins. *Schw. Mineral. Petro. Mitteil.* 74, 383–401.
- Irving, A.J., Frey, F.A., 1978. Distribution of trace elements between garnet megacrysts and host volcanic liquids of kimberlitic to rhyolitic composition. *Geochim. Cosmochim. Acta* 42, 771–787.
- Klaver, M., Smeets, R.J., Koornneef, J.M., Davies, G.R., Vroon, P.Z., 2016. Pb isotope analysis of ng size samples by TIMS equipped with a $10^{13} \Omega$ resistor using a ^{207}Pb - ^{204}Pb double spike. *J. Anal. At. Spectrom.* 31, 171–178.
- Klemme, S., O'Neill, H.S.C., 2000. The near-solidus transition from garnet lherzolite to spinel lherzolite. *Contrib. Mineral. Petrol.* 138, 237–248.
- Krmčková, S., Krmčák, L., Romer, R.L., Ulrych, J., 2020. Lead isotope evolution of the Central Europe upper mantle: Constraints from the Bohemian Massif. *Geosci. Front.* 11, 925–942.
- Laurent, O., Couzinié, S., Zeh, A., Vanderhaeghe, O., Moyen, J.F., Villaros, A., Gardien, V., Chelle-Michou, C., 2017. Protracted, coeval crust and mantle melting during Variscan late-orogenic evolution: U-Pb dating in the eastern French Massif Central. *Int. J. Earth Sci.* 106, 421–451.
- Li, C.-F., Chen, F., Li, X.-H., 2007. Precise isotopic measurements of sub-nanogram Nd of standard reference material by thermal ionization mass spectrometry using the NdO⁺ technique. *Int. J. Mass Spectrom.* 266, 34–41.
- Lierenfeld, M.B., Mattsson, H.B., 2015. Geochemistry and eruptive behaviour of the Finca La Nava maar volcano (Campo de Calatrava, south-Central Spain). *Int. J. Earth Sci.* 104, 1795–1817.
- López-Moro, F.J., López-Plaza, M., 2004. Monzonitic series from the Variscan Tormes Dome (Central Iberian Zone): petrogenetic evolution from monzogabbro to granite magmas. *Lithos* 72, 19–44.
- López-Moro, J., Murciego, A., López-Plaza, M., 2007. Silurian/Ordovician asymmetrical sill-like bodies from La Codosera syncline, W Spain: a case of tholeiitic partial melts emplaced in a single magma pulse and derived from a metasomatized source. *Lithos* 96, 567–590.
- López-Moro, J., Romer, R.L., López-Plaza, M., González-Sánchez, M., 2017. Zircon and allanite U-Pb ID-TIMS ages of vaugnerites from the Calzadilla pluton, Salamanca (Spain): dating mantle-derived magmatism and post-magmatic subsolidus overprint. *Geol. Acta* 15, 395–408.
- Lustrino, M., Wilson, M., 2007. The circum-Mediterranean anorogenic Cenozoic igneous province. *Earth Sci. Rev.* 81, 1–65.
- Lustrino, M., Fedele, L., Agostini, S., Prelevic, D., Salari, G., 2019. Leucitites within and around the Mediterranean area. *Lithos* 324–325, 216–233.
- Martínez Catalán, J.R., Rubio Pascual, F.J., Díez Montes, A., Díez Fernández, R., Gómez Barreiro, J., Dias da Silva, I., González Clavijo, E., Ayarza, P., Alcock, J.E., 2014. The late Variscan HP/LP metamorphic event in NW and Central Iberia: relationships to crustal thickening, extension, orovline development and crustal evolution. In: Schulmann, K., Martínez Catalán, J.R., Lardeaux, J.M., Janousek, V., Oggiano, G. (Eds.), *The Variscan Orogeny: Extent, Timescale and the Formation of the European Crust*, 405. *Geol. Soc. London, Spec. Publ.* pp. 225–247.
- Martins, L.T., Kerrich, R., 1998. Magmatismo toleítico continental no Algarve (Sul de Portugal): Um exemplo de contaminação cristal “in situ”. *Comun. Inst. Geol. Mineiro* 85, 99–116.
- Martins, L.T., Madeira, J., Youbi, N., Munhá, J., Mata, J., Kerrich, R., 2008. Rift-related magmatism of the Central Atlantic magmatic province in Algarve, Southern Portugal. *Lithos* 101, 102–124.
- Mata, J., Alves, C.F., Martins, L., Miranda, R., Madeira, J., Pimentel, N., Martins, S., Azevedo, M.R., Youbi, N., De Min, A., Almeida, I.M., Bensalah, M.K., Terrinha, P., 2015. $^{40}\text{Ar}/^{39}\text{Ar}$ ages and petrogenesis of the West Iberia margin onshore magmatism at the Jurassic-cretaceous transition: Geodynamic implications and assessment of open system processes involving saline materials. *Lithos* 236–237, 156–172.
- McKenzie, D., O’Nions, R.K., 1991. Partial melt distributions from inversion of rare earth element concentrations. *J. Petrol.* 32, 1021–1091.
- Merino Martínez, E., Villaseca, C., Orejana, D., Pérez-Soba, C., Belousova, E., Andersen, T., 2014. Tracing magma sources of three different S-type peraluminous granitoid series by in situ U-Pb geochronology and Hf isotope zircon composition: the Variscan Montes de Toledo batholith (Central Spain). *Lithos* 200–201, 273–298.
- Michard, A., Gurriet, P., Soudant, M., Albarede, F., 1985. Nd isotopes in French Phanerozoic shales: external vs internal aspects of crustal evolution. *Geochim. Cosmochim. Acta* 49, 601–610.
- Miranda, R., Valadares, V., Terrinha, P., Mata, J., Azevedo, M.R., Gaspar, M., Kullberg, J. C., Ribeiro, C., 2009. Age constraints on the late cretaceous alkaline magmatism on the Western Iberian Margin. *Cretac. Res.* 30, 575–586.
- Najih, A., Montero, P., Verati, C., Chabou, M.C., Fekkak, A., Baïdder, L., Ezzouhairi, H., Bea, F., Michard, A., 2019. Initial Pngean rifting north of the West African Craton: insights from late Permian U-Pb and $^{40}\text{Ar}/^{39}\text{Ar}$ dating of alkaline magmatism from the Eastern Anti-Atlas (Morocco). *J. Geodyn.* 132, 101670.
- Orejana, D., Villaseca, C., Billström, K., Paterson, B.A., 2008. Petrogenesis of Permian alkaline lamprophyres and diabases from the Spanish Central System and their geodynamic context within western Europe. *Contrib. Mineral. Petrol.* 156, 457–500.
- Orejana, D., Villaseca, C., Pérez-Soba, C., López-García, J.A., Billström, K., 2009. The Variscan gabbros from the Spanish Central System: a case for crustal recycling in the sub-continental lithospheric mantle? *Lithos* 110, 262–276.
- Orejana, D., Villaseca, C., Valverde-Vaquero, P., Belousova, E.A., Armstrong, R.A., 2012. U-Pb geochronology and zircon composition of late Variscan S- and I-type granitoids from the Spanish Central System batholith. *Int. J. Earth Sci.* 101, 1789–1815.
- Orejana, D., Villaseca, C., Merino Martínez, E., 2017. Basic Ordovician magmatism of the Spanish Central System: Constraints on the source and geodynamic setting. *Lithos* 284–285, 608–624.
- Orejana, D., Villaseca, C., Kristoffersen, M., 2020. Geochemistry and geochronology of mafic rocks from the Spanish Central System: Constraints on the mantle evolution beneath Central Spain. *Geosci. Front.* 11, 1651–1667.
- Palencia Ortas, A., Osete, M.L., Vegas, R., Silva, P., 2006. Paleomagnetic study of the Messejan Plasencia dyke (Portugal and Spain): a lower Jurassic paleopole for the Iberian plate. *Tectonophysics* 420, 455–472.
- Palomeras, I., Ayarza, P., Andrés, J., Álvarez-Valero, A.M., Gómez-Barreiro, J., Díaz, J., Alcalde, J., Carbonell, R., 2021. Mapping and interpreting the uppermost mantle reflectivity beneath central and south-west Iberia. *J. Geophys. Res. Solid Earth* 126, e2020JB019987.
- Pearce, J.A., 1982. Trace elements characteristics of lavas from destructive plate boundaries. In: Thorpe, R.S. (Ed.), *Andesites*. Wiley, Chichester, pp. 525–548.
- Pearce, J.A., 1996. A users guide to basalt discrimination diagrams. In: Wyman, D.A. (Ed.), *Trace element Geochemistry of Volcanic Rocks: Applications For Massive Sulphide Exploration*, 12. *Geol. Assoc. Canada, Short Course Notes*, pp. 79–113.
- Pearce, J.A., 2014. Immobile element fingerprinting of ophiolites. *Elements* 10, 101–108.
- Peccerillo, A., 2017. Cenozoic Volcanism in the Tyrrhenian Sea Region, 2nd edition. Springer International Publishing, p. 399.
- Pérez-Cáceres, I., Martínez Poyatos, D., Simancas, J.F., Azor, A., 2015. The elusive nature of the Rheic Ocean suture in SW Iberia. *Tectonics* 34, 2429–2450.
- Pérez-Cáceres, I., Simancas, J.F., Martínez Poyatos, D., Azor, A., González Lodeiro, F., 2016. Oblique collision and deformation partitioning in the SW Iberian Variscides. *Solid Earth* 7, 857–872.
- Pfänder, J.A., Jung, S., Klügel, A., Münker, C., Romer, R.L., Sperner, B., Rohrmüller, J., 2018. Recurrent local melting of metasomatized lithospheric mantle in response to continental rifting: constraints from basanites and nephelinites/mellilitites from SE Germany. *J. Petrol.* 59, 667–694.
- Prelevic, D., Foley, S.F., Romer, R., Conticelli, S., 2008. Mediterranean Tertiary lamproites derived from multiple source components in postcollisional geodynamics. *Geochim. Cosmochim. Acta* 72, 2125–2156.
- Puelles, P., Gil Ibarguchi, J.L., García de Madinabeitia, S., Sarriónandia, F., Carracedo-Sánchez, M., Fernández-Armas, S., 2019. Granulite-facies gneisses and meta-igneous xenoliths from the Campo de Calatrava volcanic field (Spain). Implications for the tectonics of the Variscan lower crust. *Lithos* 342–343, 114–134.
- Puziewicz, J., Matusiak-Malek, M., Ntafos, T., Grégoire, M., Kaczmarek, M.-A., Aulbach, S., Ziobro, M., Kukulka, A., 2020. Three major types of subcontinental mantle beneath the Variscan orogeny in Europe. *Lithos* 362–363, 105467.
- Quesada, C., 1991. Geological constraints on the Paleozoic tectonic evolution of the tectonostratigraphic terranes in the Iberian Massif. *Tectonophysics* 185, 225–245.
- Ribeiro, A., Munhá, J., Dias, R., Mateus, A., Pereira, L., Fonseca, P., Araújo, A., Oliveira, T., Romão, J., Chaminé, H., Coke, C., Pedro, J., 2007. Geodynamic evolution of the SW Europe Variscides. *Tectonics* 26, TC6009 (24 pp.).
- Ribeiro, A., Munhá, J., Fonseca, P., Araújo, A., Pedro, J., Mateus, A., Tassinari, C., Machado, G., Jesus, A., 2010. Variscan ophiolite belts in the Ossa-Morena Zone (Southwest Iberia): Geological characterization and geodynamic significance. *Gondwana Res.* 17, 408–421.
- Rodríguez-Alonso, M.D., Peinado, M., López-Plaza, M., Franco, P., Carnicero, A., Gonzalo, J.C., 2004. Neoproterozoic-Cambrian syndesimatory magmatism in the Central Iberian Zone (Spain): geology, petrology and geodynamic significance. *Int. J. Earth Sci.* 93, 897–920.
- Rollinson, H., 1993. *Using Geochemical Data: Evaluation, Presentation, Interpretation*. Longman Scientific & Technical, Singapore, p. 352.
- Ross, M.E., 2010. An Early Triassic $^{40}\text{Ar}/^{39}\text{Ar}$ age for a camptonite dyke in Cambridge, Massachusetts. *Atl. Geol.* 46, 127–135.
- Roubardet, M., Gutiérrez-Marco, J.C., 2002. Silurian. In: Gibbons, W., Moreno, T. (Eds.), *The Geology of Spain*. *Geol. Soc., London*, pp. 51–66.
- Rubio-Ordóñez, A., Valverde-Vaquero, P., Corretgé, L.G., Cuesta, A., Gallastegui, G., Fernández-González, M., Gerdes, A., 2012. An early Ordovician tonalitic-granodioritic belt along the Schistose-Greywacke Domain of the Central Iberian Zone (Iberian Massif, Variscan Belt). *Geol. Mag.* 149, 927–939.
- Rudnick, R., Gao, S., 2005. Composition of the continental crust. *Treatise Geochem.* 3, 1–64.
- Sánchez García, T., Chichorro, M., Solá, A.R., Álvaro, J.J., Díez-Montes, A., Bellido, F., Ribeiro, M.L., Quesada, C., Lopes, J.C., Dias da Silva, I., González-Clavijo, E., Gómez Barreiro, J., López-Carmona, A., 2019. The Geology of Iberia: A Geodynamic Approach. In: Quesada, C., Oliveira, J.T. (Eds.), *The Variscan Cycle*. Regional Geology Reviews, Vol. 2. Springer Nature Switzerland AG 2019, pp. 27–74.
- Scarrow, J.H., Molina, J.F., Bea, F., Montero, P., 2009. Within-plate calc-alkaline rocks: Insights from alkaline mafic magma-peraluminous crustal melt hybrid appinites of the Central Iberian Variscan continental collision. *Lithos* 110, 50–64.
- Scarrow, J.H., Molina, J.F., Bea, F., Montero, P., Vaughan, A.P.M., 2011. Lamprophyre dikes as tectonic markers of late orogenic transtension timing and kinematics: a case study from the Central Iberian Zone. *Tectonics* 30, TC4007.

- Schermerhorn, L.J.G., Priem, H.N.A., Boelrijk, N.A.I.M., Hebeda, E.H., Verdurmen, E.A. Th, Verschure, R.H., 1978. Age and origin of the Mesejana dolerite fault-dike system (Portugal and Spain) in the light of the opening of the North Atlantic Ocean. *J. Geol.* 86, 299–309.
- Schmidt, K.H., Botazzi, P., Vannucci, R., Mengel, K., 1999. Trace element partitioning between phlogopite, clinopyroxene and leucite lamproite melt. *Earth Planet. Sci. Lett.* 168, 287–299.
- Shaw, D.M., 1970. Trace element fractionation during anatexis. *Geochim. Cosmochim. Acta* 34, 237–243.
- Solá, A.R., Neiva, A.M.R., Ribeiro, M.L., Moreira, M.E., 2003. Geochemistry of igneous rocks from Carrascal Massif (Central Portugal): a preliminary approach. *J. Czech Geol. Soc.* 48, 115–116.
- Solá, A.R., Pereira, M.F., Williams, I.S., Ribeiro, M.L., Neiva, A.M.R., Montero, P., Bea, F., Zinger, T., 2008. New insights from U-Pb zircon dating of early Ordovician magmatism on the northern Gondwana margin: the Urro Formation (SW Iberian Massif, Portugal). *Tectonophysics* 461, 114–129.
- Solá, A.R., Neiva, A.M.R., Ribeiro, M.L., 2010. Geocronologia, petrologia e geoquímica dos granitóides do NE Alentejano (transição ZCI/ZOM): significado geodinâmico. In: *Ciências Geológicas-Ensino e Investigação e sua História*, vol. I, pp. 281–290. Cap. II. <http://repositorio.ineg.pt/bitstream/10400.9/1270/1/34381.pdf>.
- Stagno, V., Stopponi, V., Kono, Y., Manning, C.E., Irifune, T., 2018. Experimental determination of the viscosity of Na_2CO_3 melt between 1.7 and 4.6 GPa at 1200–1700 °C: Implications for the rheology of carbonatite magmas in the Earth's upper mantle. *Chem. Geol.* 501, 19–25.
- Stampfli, G.M., Hochard, C., Vérard, C., Wilhelm, C., von Raumer, J., 2013. The formation of Pangea. *Tectonophysics* 593, 1–19.
- Sun, S., McDonough, W.F., 1989. Chemical and isotopic systematics of oceanic basalts: implications for mantle and processes. In: Saunders, A.D., Norry, M.J. (Eds.), *Magmatism in the Ocean Basins*, 42. Geol. Soc., London, Spec. Publ., pp. 313–345.
- Thöni, M., Miller, C., 2009. The “Permian event” in the eastern European Alps: Sm-Nd and P-T data recorded by multi-stage garnet from the Plankogel unit. *Chem. Geol.* 260, 20–36.
- Uenver-Thiele, L., Woodland, A.B., Steiz, H.-M., Downes, H., Altherr, R., 2017. Metasomatic processes revealed by trace element and redox signatures of the lithospheric mantle beneath the Massif Central, France. *J. Petrol.* 58, 395–422.
- Van Hinsbergen, D.J.J., Torsvik, T.H., Schmid, S.M., Matenço, L.C., Maffione, M., Vissers, R.L.M., Gürer, D., Spakman, W., 2020. Orogenic architecture of the Mediterranean region and kinematic reconstruction of its tectonic evolution since the Triassic. *Gondwana Res.* 81, 79–229.
- Verati, C., Rapaille, C., Féraud, G., Marzoli, A., Bertrand, H., Youbi, N., 2007. $^{40}\text{Ar}/^{39}\text{Ar}$ ages and duration of the Central Atlantic Magmatic Province volcanism in Morocco and Portugal and its relation to the Triassic-Jurassic boundary. *Palaeogeogr. Palaeoclimatol. Palaeoecol.* 244, 308–325.
- Villaseca, C., Downes, H., Pin, C., Barbero, L., 1999. Nature and composition of the lower continental crust in Central Spain and the granulite-granite linkage: inferences from granulitic xenoliths. *J. Petrol.* 40, 1465–1496.
- Villaseca, C., Orejana, D., Pin, C., López-García, J.A., Andonaegui, P., 2004. Le magmatisme basique hercynien et post-hercynien du Système Central Espagnol: essai de caractérisation des sources mantelliques. *Compt. Rendus Geosci.* 336, 877–888.
- Villaseca, C., Bellido, F., Pérez-Soba, C., Billström, K., 2009. Multiple crustal sources for post-tectonic I-type granites in the Hercynian Iberian Belt. *Mineral. Petrol.* 96, 197–211.
- Villaseca, C., Ancochea, E., Orejana, D., Jeffries, T.E., 2010. Composition and evolution of the lithospheric mantle in Central Spain: inferences from peridotite xenoliths from the Cenozoic Calatrava volcanic field. *Geol. Soc. Spec. Publ.* 337, 125–151.
- Villaseca, C., Orejana, D., Belousova, E.A., Armstrong, R.A., Pérez-Soba, C., Jeffries, T.E., 2011. U-Pb isotopic ages and Hf isotope composition of zircons in Variscan gabbros from Central Spain: evidence of variable crustal contamination. *Mineral. Petrol.* 101, 151–167.
- Villaseca, C., Castiñeiras, P., Orejana, D., 2015. Early Ordovician metabasites from the Spanish Central System: a remnant of intraplate HP rocks in the Central Iberian Zone. *Gondwana Res.* 27, 329–409.
- Villaseca, C., Merino Martínez, E., Orejana, D., Andersen, T., Belousova, E., 2016. Zircon Hf signatures from granitic orthogneisses of the Spanish Central System: significance and sources of the Cambro-Ordovician magmatism in the Iberian Variscan Belt. *Gondwana Res.* 34, 60–83.
- Villaseca, C., Belousova, E., Barfod, D., González-Jiménez, J.M., 2019. Dating metasomatic events in the lithospheric mantle beneath the Calatrava volcanic field (Central Spain). *Lithosphere* 11, 192–208.
- Villaseca, C., García Serrano, J., Orejana, D., 2020. Pyroxenite and megacrysts from alkaline melts of the Calatrava Volcanic Field (Central Spain): Inferences from trace element geochemistry and Sr-Nd isotope composition. *Front. Earth Sci.* 8, 132.
- Villaseca, C., García Serrano, J., Pérez-Soba, C., 2022. Subduction-related metasomatism in the lithospheric mantle beneath the Calatrava volcanic field (Central Spain): constraints from lherzolite xenoliths of the Cerro Gordo volcano. *Intern. Geol. Rev.* 64, 469–488. <https://doi.org/10.1080/00206814.2020.1858453>.
- Von Raumer, J.F., Bussy, F., Scaltegger, U., Schulz, B., Stampfli, G.M., 2013. Pre-Mesozoic Alpine basements-their place in the European Paleozoic framework. *Geol. Soc. Am. Bull.* 125, 89–108.
- Weis, D., Kieffer, B., Maerschalk, C., Barling, J., de Jong, J., Williams, G.A., Hanano, D., Pretorius, W., Matielli, N., Scoates, J.S., Goolaerts, A., Friedman, R.M., Mahoney, J. B., 2006. High-precision isotopic characterization of USGS reference materials by TIMS and MC-ICP-MS. *Geochem. Geophys. Geosyst.* 7 <https://doi.org/10.1029/2006GC001283>.
- White, W.M., Albarède, F., Télouk, Ph., 2000. High precision analysis of Pb isotope ratios by multi-collector ICP-MS. *Chem. Geol.* 167, 257–270.
- Zartman, R.E., Doe, B.R., 1981. Plumbotectonics—the model. *Tectonophysics* 75, 135–162.
- Ziegler, P.A., Schumacher, M.E., Dèzes, P., Van Wees, J.D., Cloetingh, S., 2004. Post-Variscan evolution of the lithosphere in the Rhine Graben area: constraints from subsidence modelling. *Geol. Soc. London Spec. Publ.* 223, 289–317.
- Zindler, A., Hart, S.R., 1986. Chemical geodynamics. *Annu. Rev. Earth Planet. Sci.* 14, 493–571.